Chem Soc Rev

Chemical Society Reviews

www.rsc.org/chemsocrev

Volume 38 | Number 4 | April 2009 | Pages 853–1200

Published on 13 February 2009. Downloaded by Pennsylvania State University on 12/09/2016 18:00:11.

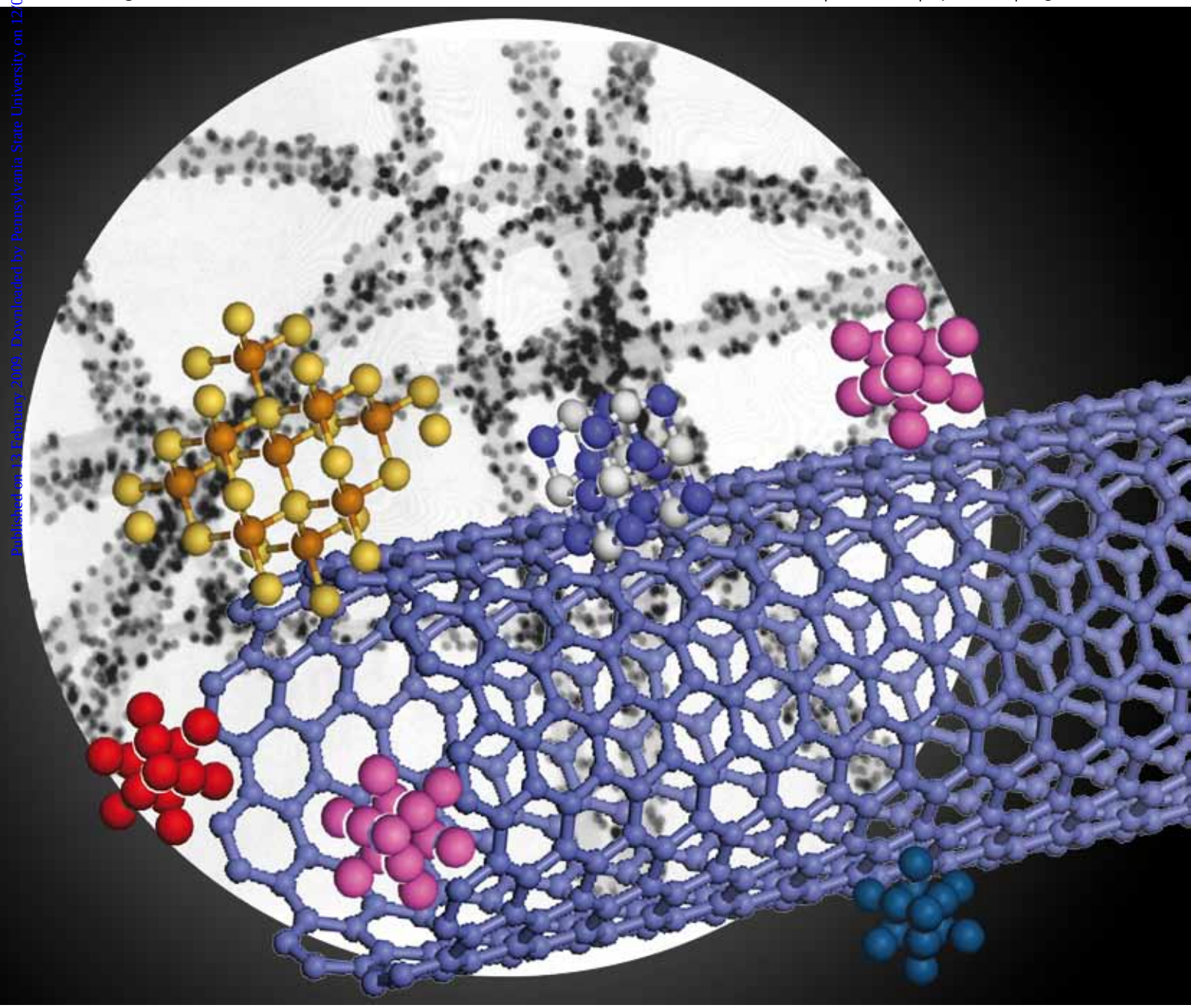

ISSN 0306-0012

CRITICAL REVIEW
Xiaohui Peng, Jingyi Chen, James A. Misewich and Stanislaus S. Wong
Carbon nanotube–nanocrystal heterostructures

TUTORIAL REVIEW
Meike Cordes and Bernd Giese
Electron transfer in peptides and proteins

RSC Publishing

Carbon nanotube–nanocrystal heterostructures

Xiaohui Peng,[a] Jingyi Chen,[b] James A. Misewich[b] and Stanislaus S. Wong*[ab]

Received 30th July 2008
First published as an Advance Article on the web 13th February 2009
DOI: 10.1039/b811424m

Published on 13 February 2009. Downloaded by Pennsylvania State University on 12/09/2016 18:00:11.

The importance of generating carbon nanotube–nanoparticle heterostructures is that these composites ought to take advantage of and combine the unique physical and chemical properties of both carbon nanotubes and nanoparticles in one discrete structure. These materials have potential applicability in a range of diverse fields spanning heterogeneous catalysis to optoelectronic device development, of importance to chemists, physicists, materials scientists, and engineers. In this *critical review*, we present a host of diverse, complementary strategies for the reliable synthesis of carbon nanotube–nanoparticle heterostructures using both covalent as well as non-covalent protocols, incorporating not only single-walled and multi-walled carbon nanotubes but also diverse classes of metallic and semiconducting nanoparticles (221 references).

1 Introduction

Carbon nanotubes[1] are the focal point of intense study because fundamentally, they are in essence a tunable, molecularly defined structure with reproducible dimensions. For instance, for single-walled carbon nanotubes (SWNTs), the combination of their helicity and diameter, defined by the roll-up vector, often determines whether a tube is a metal or a semiconductor.[2,3] Theoretical predictions from band structure calculations[4] and experimental determinations from STM measurements[5] in fact show that the band gap of semiconducting nanotubes decreases with increasing diameter. Moreover, the mechanical strength (*i.e.* buckling force) of SWNTs is a function of its length and diameter.[6,7] In general, because carbon nanotubes (CNTs) possess unique structural, electronic, mechanical, and optical properties, they are actively sought as components of devices in a variety of different fields. These include but are not limited to usage in field-effect transistors (FETs),[8] light-emitting diodes (LEDs),[9] and catalyst supports in fuel cells.[10] Additionally, the high surface area, mechanical strength, and thermal stability of these systems suggest a host of wide-ranging, potential applications including as catalyst supports in heterogeneous catalysis, field emitters, high-strength engineering fibers, sensors, actuators, components of composites, tips for scanning probe microscopy, gas storage media, and molecular wires for the next generation of electronic devices.[11–21]

Hence, a predictable understanding of the chemistry of CNTs becomes critical to the rational manipulation of their

[a] *Department of Chemistry, State University of New York at Stony Brook, NY 11794-3400 Stony Brook, USA. E-mail: sswong@notes.cc.sunysb.edu. E-mail: sswong@bnl.gov; Tel: 631-632-1703; 631-344-3178*
[b] *Condensed Matter Physics and Materials Sciences Department, Brookhaven National Laboratory, Building 480, Upton, NY 11973, USA*

Xiaohui Peng

Xiaohui Peng is currently a doctoral student in Chemistry at the State University of New York at Stony Brook, under the supervision of Prof. Stanislaus S. Wong. She earned a BSc in Chemistry from Nanjing University in 2006. Her research interests include devising new strategies for chemical functionalization of carbon nanotubes, probing the synthesis and characterization of carbon nanotube-based materials, as well as understanding the electronic and optical properties of these hybrid nanomaterials.

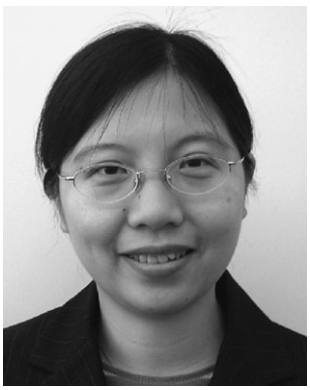

Jingyi Chen

Jingyi Chen received a BS from Sun Yat-Sen University in China (1997), a MA in chemistry with Professor Kimberly A. Bagley from SUNY College at Buffalo (2002), and a PhD in chemistry and nanotechnology with Professor Younan Xia from the University of Washington in Seattle (2006). She then worked as a postdoctoral fellow with Professor Stanislaus S. Wong at Brookhaven National Laboratory. In May 2008, she began as a Research Assistant Professor in the Department of Biomedical Engineering at Washington University in St. Louis. Her research interests include synthesis, characterization, and surface functionalization of nanomaterials for applications in catalysis, photovoltaics, and biomedical research.

 This journal is © The Royal Society of Chemistry 2009

Published on 13 February 2009. Downloaded by Pennsylvania State University on 12/09/2016 18:00:11.

properties. Specifically, if nanotubes are ever to be utilized as components of practical, macroscopic devices on a large scale, there is a complementary need for CNTs to be controllably assembled into more sophisticated and hierarchical architectures. Such a capability is key to building complex, functional nanotube devices with desirable properties. In other words, CNTs need to be arranged into spatially well-defined configurations in order to design integrated systems with predictable attributes. Though nanostructure assembly motifs can be devised based on either biological recognition or lithographic approaches, the construction of supramolecular hierarchical assemblies composed of CNTs is one task in which a fundamental understanding and application of nanotube chemistry can play a central and defining role.

In this specific critical review, we explore various strategies for creating and generating a particular architecture, namely carbon nanotube–nanocrystal heterostructures. Why nanocrystals? Nanocrystals typically possess a diameter of under <50 nm and may contain as few as a hundred or as many as tens of thousands of atoms. Semiconductor nanocrystals,[22–24] such as CdS and CdSe, alternatively known as quantum dots, exhibit strongly size-dependent optical and electrical properties, that are predictable and hence useful. Because of their 2–50 nm size range, nanocrystals are unique in that the number of surface atoms is a large fraction of the total. Hence, their intrinsic properties are transformed by quantum size effects due to the spatial confinement of excitations. The high luminescence yield of these materials as well as the potential of adjusting emission and absorption wavelengths by controllably selecting the nanocrystal size make these materials attractive as components in a wide range of optoelectronic devices (such as semiconductors and lasers). Moreover, they have been used for fluorescent labeling in biology.[25]

Generating a heterojunction incorporating both of these classes of nanostructures (namely nanotubes and nanocrystals, externally bound and connected) is therefore significant, because an individual heterostructure can conceivably possess a junction area of less than 10 nm^2, which is far smaller than any junction reliably produced thus far. The unique, innovative, and important aspect of this nanoscale architecture is that it takes advantage of the tunability, in terms of size, shape, and chemistry, of nanotubes and nanocrystals, to create a sharp junction interface, whose properties are inherently manipulable, tailorable, and hence, predictable. For example, the electrical resistance of nanotube–nanoparticle networks is dependent on the nanoscale junctions that exist between these constituent nanomaterials as well as on microscale and macroscale connectivity.[26] Thus, rational design of these nanomaterials is critical to a fundamental understanding of charge transport in single molecules and the determination of their conductance. Results on these systems can therefore be used to increase understanding of intrinsic factors affecting carrier mobility, such as electronic structure, carrier trapping, and delocalization. Knowledge of these parameters will become important if nanotubes and nanocrystals are ever to be incorporated as building blocks for future generations of molecular electronics and computational device architectures, especially complex conductor networks as well as T- and Y-junctions.[27–30]

1.2 Characterization tools

A number of analytical techniques and methodologies have been employed to not only comprehensively characterize CNT–nanocrystal heterostructures but also thoroughly investigate the properties of these CNT–nanocrystal hybrids. First, in order to identify the chemical constituents within the hybrids, X-ray diffraction (XRD) measurements offer a relatively simple, versatile, and non-destructive methodology to reveal detailed information about their chemical composition

James A. Misewich

James A. Misewich earned his PhD from Cornell University in 1984 in physical chemistry. He then joined the laser physics group at the IBM Thomas J. Watson Research Center in Yorktown Heights, NY. In 2002, he came to Brookhaven as Chair of the Materials Science Department and later became Chair of the Condensed Matter Physics and Materials Science Department. In June 2007, he became Interim Associate Laboratory Director, a position he held until his current appointment as Associate Laboratory Director for Basic Energy Sciences. He has made significant contributions in several fields, including optics, nanomaterials, ultrafast studies, and surface science.

Stanislaus S. Wong

Stanislaus S. Wong earned a BSc (First Class Honours) from McGill University in 1994, and a PhD from Harvard University in 1999 under the tutelage of Professor Charles M. Lieber. After completing a postdoctoral fellowship at Columbia University with Professor Louis E. Brus, he initially held the position of Assistant Professor (2000–2006), and was promoted to Associate Professor (September 2006–present) in Chemistry at SUNY Stony Brook with a joint appointment at Brookhaven National Laboratory. His research includes the rational chemical functionalization of carbon nanotubes and the synthesis and characterization of non-carbonaceous nanostructures. Professor Wong has earned a National Science Foundation CAREER award, as well as an Alfred P. Sloan Foundation Faculty Fellowship.

Published on 13 February 2009. Downloaded by Pennsylvania State University on 12/09/2016 18:00:11.

as well as crystallographic structure and phase. Coupled with electron diffraction, a characteristic X-ray diffraction pattern would not only allow the precise identification of nanocrystals but also confirm the existence of nanocrystals within the hybrids themselves. In addition, elements associated with specific localized regions within the heterostructures themselves could also be identified and verified using energy dispersive X-ray spectroscopy (EDS). X-Ray photoelectron spectroscopy (XPS), a widely used quantitative spectroscopic technique, has also been applied to measure elemental composition, the nature of chemical bonding states, and electronic structures of elements within these CNT–nanocrystal hybrids. Mid-infrared spectroscopy has also assisted in confirming the successful functionalization and bonding of nanocrystals to CNTs in the presence of intermediary linkers, polymer chains, or polyelectrolytes with distinctive chemical signatures.

Second, transmission electron microscopy (TEM) and scanning electron microscopy (SEM) represent the most straightforward methodologies for visually inspecting the morphology and structure of CNT–nanocrystal hybrids, by which the shape and size of nanocrystals as well as the density and distribution of nanocrystals on the CNTs themselves can be accurately observed and determined. Moreover, high-resolution TEM (HRTEM) can yield information about lattice planes and *d*-spacings of components within the heterostructure. Examining adjoining lattice layers of nanotubes and nanocrystals can reveal insights into the growth mechanism of nanocrystals on the CNT surface as well as the associated effects of CNTs on the subsequent morphology of *in situ* grown nanocrystals. For instance, it has been demonstrated that hexagonal phase β-Cu_2S nanoplates can be grown *in situ* on acid-functionalized MWNTs by the solvothermal method; the lattice matching between the (002) planes of Cu_2S and the (002) planes of the MWNTs was thought to be an important factor in the growth of the Cu_2S nanocrystals.[31] Alternatively, atomic force microscopy (AFM), a very high-resolution scanning probe microscopy technique, can be used to provide real-time height information about non-conducting samples in a wide variety of different sample environments (including air, vacuum, and liquid) and the resulting three-dimensional surface profiles of CNT–nanocrystal heterostructures, thus obtained, can complement data derived from electron microcopy.

Third, near-infrared (NIR) spectroscopy (4000–12500 cm^{-1}) has been promoted as an efficient tool to characterize the electronic structure of SWNTs due to the unique spectroscopic features resulting from interband electronic transitions between pairs of van Hove singularities[32–34] in either semiconducting or metallic SWNTs. The technique has been extensively used to evaluate the effect of covalent chemistry on band structure, thereby providing an excellent opportunity to probe the coupling of nanocrystals with the electronic structure of CNTs. For example, the disappearance of electronic transitions and accompanying flattening of spectral features in the UV-visible-NIR range is often indicative of the perturbation of electronic structure of CNTs.[35] Similarly, Raman spectroscopy is a particularly sensitive probe of electronic and vibrational structure and their coupling in SWNTs.[36] Characteristic features of the Raman spectrum of SWNTs include the diameter-dependent radial breathing modes (RBM)[37] (150–300 cm^{-1}), the tangential mode or G band (~1560–1600 cm^{-1}), and the disorder-induced D band (~1290–1320 cm^{-1}). Importantly, the shape and intensity of a disorder mode peak has been correlated with the extent of nanotube sidewall functionalization.[33,38] Sidewall functionalization of CNTs with nanocrystals is often accompanied by the formation of sp^3 hybridized carbons on the sidewalls and therefore substantial disruption of electronic structure. This can lead to a significant increase in the intensity of disorder band and that is often used as a probe for site specificity and selectivity of a functionalization reaction.[33,39,40] In general, though, with increasing extent of sidewall functionalization, as the pseudo-1-D lattice becomes increasingly disrupted, the nanotubes are no longer in electronic resonance and thus, the observed intensity of all of the peaks sharply decreases.[38]

Last but not least, on account of the unique optical properties of semiconducting nanoparticles (*e.g.* ZnO and TiO_2) and of quantum dot nanocrystals (*e.g.* CdSe, CdS and PbSe), additional techniques including UV absorption spectroscopy,[41] photoluminescence spectroscopy,[42] and fluorescence microscopy[43] already play a significant role in analyzing the optoelectronic performance of heterostructures integrating optically active nanocrystals as well as investigating charge transfer and energy transfer behavior between carbon nanotubes and nanocrystals. For example, the photoluminescent lifetime and intensity of quantum dots tend to be reduced after conjugation to SWNTs, a phenomenon related to Förster resonance energy transfer involving nonradiative energy transfer from a photoexcited quantum dot energy donor to a nearby SWNT energy acceptor in its ground state.[42] In another instance, the plasmon resonance of gold nanoparticles electrodeposited onto SWNTs effectively enhances both the particles' fluorescence as well as the local Raman response of the tubes.[44] In addition, surface photovoltage spectroscopy (SPS), a highly sensitive tool that probes the photophysics of photogenerated species as well as the excited states and band gaps of semiconductors,[45] has been developed as a novel approach to investigate photoinduced processes, such as charge transfer[46,47] and photocatalysis.[48] Based on the principle of SPS, upon illumination, electron hole pairs are generated and either recombine or dissociate into free carriers under the influence of the applied field. Movement of photogenerated electrons and holes results in a change of the surface net charge, producing a surface photovoltage whose intensity is directly proportional to the density of these surface charges. For the CNT/CdS core–shell heterostructure, it was found that the surface photovoltage response was enhanced as compared with that measured for CdS nanocrystals alone. That observation not only suggested a highly efficient photoinduced charge transfer process between CdS and the CNT but also a rather effective dissociation of photogenerated species within the CNT/CdS core–shell nanowire structure.[47]

2 Synthesis of nanotube–nanocrystal heterostructures

Not surprisingly then, the synthesis of carbon nanotube–nanocrystal heterostructures has received an ever-increasing

 This journal is © The Royal Society of Chemistry 2009

Published on 13 February 2009. Downloaded by Pennsylvania State University on 12/09/2016 18:00:11.

interest in recent years. One of the first ideas was to use nanocrystals as a means of labeling defect sites, in terms of density, distribution, and location, on SWNTs.[49] Since then, the main motivating factor for probing this synthesis has been the desire to retain the favorable properties, such as mechanical flexibility or catalytic efficiency,[50] of each constituent nanomaterial without losing out on the structural integrity and robustness of the overall heterostructure. A number of different strategies have therefore been put forward for the fabrication of CNT–nanocrystal nanocomposites. Nonetheless, these fall into two basic classes. One main approach involves the prior synthesis of nanoparticles that are then subsequently connected to functionalized CNTs *via* either covalent (*i.e.* organic or biomolecular linkers) or noncovalent interactions. The second key approach involves direct deposition of nanoparticles onto the surface of CNTs, either through formation of nanoparticles *in situ*, a reduction reaction, or an electrodeposition process using CNTs as templates. Of particular interest has been the integration of CNTs with different types of nanoparticles including noble metal nanoparticles and semiconducting quantum dots through electrostatic types of interactions. In this critical review, we explore each of these strategies with a number of salient examples, and discuss a few key, relevant applications at the end. We do not cover nanotube filling strategies herein as that area is beyond the scope of our discussion.

2.1 Covalent approaches

Modifying the CNT surface using functional groups containing desirable, pendant moieties has been an important and popular method for creating CNT-based hybrid nanostructures. There are several advantages to this particular approach. First, the shape and size of individual nanoparticles or nanocrystals can be easily tailored by sophisticated synthesis methods prior to combination with CNTs, thereby avoiding the influence of CNTs on the nucleation and growth processes of either nanoparticles or quantum dots. Second, covalent bonds can rigidly connect the linker molecules and CNTs in a reliable and robust manner, such that the nanoparticles will not become easily dislodged even after either sonication or extensive washing. Third, the spatial coverage and exact positions of either nanoparticles or nanocrystals depend on the precise nature of the chemical functionalities on the CNT surfaces, and these can be reasonably governed by controlling oxidation treatments and/or chemical reaction conditions.

In recent years, there have been a large number of reports describing the chemical modification of carbon nanotubes *via* the covalent coupling of an increasingly wide range of functional molecules and biomolecules onto the surfaces of carboxylic acid-modified CNTs. In principle, to adjoin the nanoparticles, the major coupling reaction can occur *via* a biochemically popular carbodiimide reaction leading to the formation of either amide or ester bonds. Not surprisingly, additional research in this area has focused on the synthesis of CNT–nanoparticle heterostructures[51–53] through the use of other families of organic molecular linkers or through biomolecular recognition modules involving either DNA[54] or biotin-streptavidin.[42,55] Typical examples of these various methodologies follow.

2.1.1 Mediation of an organic molecular linker. Pre-treated, 'activated' oxidized SWNTs have been attached to Au nanoparticles[51] using a 2-aminoethanethiol linker. AFM height imaging demonstrated that the amine-terminated gold colloidal particles attached to the nitric acid refluxed tubes primarily at defect sites and tips, whereas no colloidal attachment was observed using non-oxidized tubes. For CdSe attachment, the initial strategy[52] reported was slightly modified. In particular, SWNTs were pre-treated and oxidized using a permanganate-sulfuric acid mixture. Subsequent reaction with mercaptocarboxylic-capped CdSe nanocrystals in the presence of an intermediary organic linker, such as ethylenediamine, led to the formation of amide bonds in the presence of a carbodiimide such as either EDC (*N*-(3-dimethylaminopropyl)-*N*′-ethylcarbodiimide) or dicyclohexylcarbodiimide (DCC). The approach is extendable to other chalcogenide nanocrystals, such as CdTe, as well as to other classes of metal oxide nanocrystals, such as TiO_2, even though it was found that the presence of the intermediary linker was not especially necessary in the latter case. TEM results indicated that the nanocrystals tended to be concentrated at the ends and defect sites of SWNTs where the largest concentrations of carboxylic groups were present. Similarly, Ravindran *et al.*[56] demonstrated that amine-terminated ZnS-capped CdSe nanoparticles could be attached to the ends of oxidized multiwalled carbon nanotubes (MWNTs) using EDC.

It is noteworthy that additional reactions, apart from conventional coupling processes involving EDC, such as the Bingel reaction,[57] also have been utilized to sidewall functionalize CNTs with nanoparticles such as 5 nm gold colloids. It also has been claimed that the lengths of the SWNTs themselves may have an impact on whether the quantum dots bind at the ends or the sidewalls.[58] By analogy, by making use of sidewall protection using a polystyrene matrix, selective bifunctionalization of the ends of CNTs with carboxylate groups at one end and thiol groups at the other was elegantly demonstrated.[59] Specifically, in that case, the average nanoparticle density decreased from around 526 particles per micrometer near the nanotube tips to negligible values at locations beyond 700 nm from these tip regions.

As previously mentioned, nanotube-semiconducting nanocrystal composites are interesting model systems for photoelectrochemical cells, light emitting devices, and other types of photonic applications. The photocurrent in these systems originates from photoexcitation of the semiconducting quantum dots, yielding an electron–hole pair. To maximize the photocurrent requires efficient charge separation. Carbon nanotubes attached to the semiconducting nanoparticles may therefore facilitate photocurrent generation by trapping conduction band electrons, a process that results in more efficient charge separation and retardation of the recombination process. In these systems, the nanotubes act as electron acceptors while the nanoparticles can be considered as electron donors.

With CdSe/CNT heterostructures for example, Pan *et al.* noted that carbon nanotubes with different surface functional

Published on 13 February 2009. Downloaded by Pennsylvania State University on 12/09/2016 18:00:11.

groups (*i.e.* carboxyl, hydroxyl and amine) quenched the luminescence of the CdSe quantum dots to different degrees, though a higher concentration of tubes necessarily led to a decrease in PL intensity of the dots.[60] In analogous experiments, Cho *et al.*[53] obtained a high density of PbSe nanocrystals on the surfaces of SWNTs. The SWNTs were initially carboxylated by a mixture of nitric acid and sulfuric acid, and subsequently thiolated with 2-aminoethanethiol in the presence of EDC. The large number of available thiol groups resulted in a relatively high-density coverage of PbSe quantum dots (up to 20 wt%). This SWNT–PbSe complex showed a significant enhancement of external quantum efficiency of 2.6% *vs.* the 1.2% value for isolated quantum dots, presumably due to efficient harvesting of IR photons, followed by fast charge transfer and enhanced conduction within the SWNT network, which itself provided for a low-percolation-threshold dc conduction path.

2.1.2 Mediation using biomolecules. Derivatization of CNTs with biomolecules is an emerging field of research. It has been demonstrated, for example, that DNA nanostructures can be used as scaffolds themselves to organize 5 nm gold nanoparticles into arrays,[61] where the center-to-center interparticle spacing between neighboring particles is controlled to be ~38 nm. Not surprisingly, linear Au nanoparticle assemblies have been constructed using DNA-wrapped SWNTs.[62] This strategy involved an initial sonication of SWNTs in the presence of thiolated DNA strands followed by incubation with Au nanoparticles to form rigid linear arrays of these nanocrystals, a process associated with bonding to the thiol groups enmeshed within the DNA strands that were tightly wrapping around the SWNTs. In another experiment,[54] the sidewalls of vertically aligned MWNTs were functionalized using azide photochemistry, DNA oligonucleotides were then synthesized *in situ* to render water-soluble nanotubes, and Au nanoparticles were subsequently attached using complementary DNA strands. In a third example (Fig. 1), pristine and oxidized SWNTs were attached to streptavidin-derivatized quantum dots (Str–QDs),[55] and these biologically relevant, luminescent nanotubes were subsequently visualized using conventional TEM and fluorescent microscopy.

The importance of using biomolecules as linkers is that nanoparticles can be selectively attached onto CNT templates through well-known, highly specific recognition affinity processes between biomolecules, such as streptavidin-biotin and DNA hybridization interactions. For example, streptavidin-coated gold nanoparticles have been attached to biotin-modified SWNTs in solution in a self-assembly process.[63] Such strategies have been used to facilitate internalization of nanotubes into Jurkat T leukemia cells by multivalent CD3 receptor-mediated endocytosis.[55] Very recently, more precise structures, involving 1.4 nm gold nanoparticles, have been controllably organized onto nanotube sidewalls in one-dimensional arrays with a spacing of 2.6 nm, implying an underlying protein-directed organization process, based on molecular recognition.[64] Multilayer, multifunctional CNT-based aggregates[65] have been constructed stepwise by exploiting specific recognition processes such as

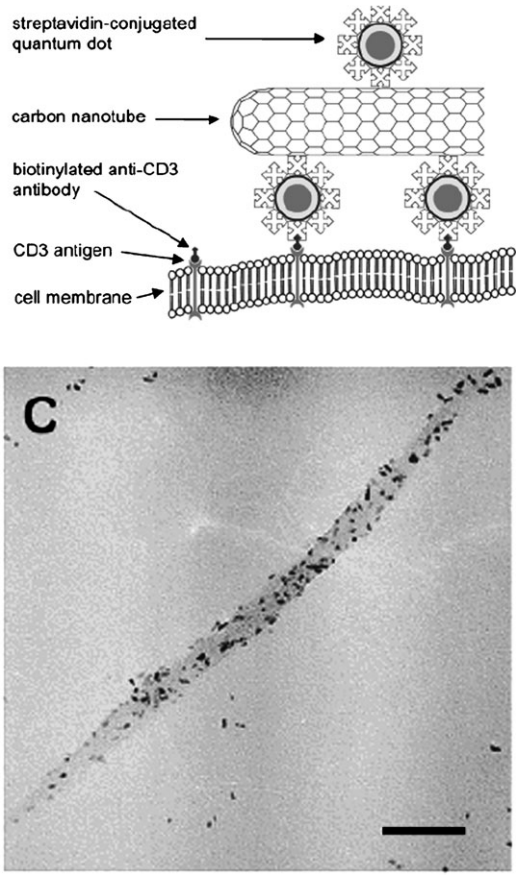

Fig. 1 (Top) Schematic showing the interactions between CD3 receptors on the Jurkat T leukemia cell membrane and a SWNT–streptavidin–quantum dot nanoassembly. A biotinylated anti-CD3 monoclonal antibody was used to link CD3 to the nanoassembly. The supramolecular luminescent nanoassembly acted as a multivalent delivery system, with each nanoassembly capable of binding many biotinylated αCD3–CD3 receptor complexes. (Bottom) TEM image of a rope of SWNT coated by Str-QD (scale bar 100 nm). Reprinted with permission from M. Bottini, F. Cerignoli, M. I. Dawson, A. Magrini, N. Rosato and T. Mustelin, *Biomacromolecules*, 2006, **7**, 2259. Copyright 2006, American Chemical Society.

biotin-streptavidin binding or DNA duplexation. These interactions have been exploited for reversible assembly and disassembly of the oligonucleotide-derivatized Au nanoparticle layer. Finally, even engineered viruses[66] have been used to assist in the assembly of an array of hybrid nanotube–quantum dot structures.

2.1.3 Summary of covalent approaches. The beauty of these reactions is that well-defined, structurally characterizable chemical bonds between the nanotubes and nanocrystals are formed. It is evident that covalent protocols clearly present a viable route towards creating robust conjugates of carbon nanotubes with nanocrystals. A wide range of different types of readily available and known linkers, including either organic molecules or biomolecules, can be chosen to bridge carbon nanotubes with nanocrystals, depending on the intrinsic requirements of the desired heterostructure, thereby highlighting the inherent flexibility of this approach. In particular, biomolecules offer advantages of not only highly

 This journal is © The Royal Society of Chemistry 2009

Published on 13 February 2009. Downloaded by Pennsylvania State University on 12/09/2016 18:00:11.

specific recognition affinity but also biocompatibility, which are prerequisites for the creation of functional, biologically relevant nanoscale devices. Finally, as the relative separation between nanotubes and nanocrystals (especially quantum dots) is practically dependent upon the nature and size of the linkers involved and is therefore a tunable parameter through relevant synthesis, for example, one has a viable means of influencing either energy transfer or charge transfer between the two components within the heterostructure. This remains a focal point of much current investigation.

2.2 Non-covalent approaches. It has been noted that one of the consequences of covalent functionalization of CNTs is to convert sp^2-hybridized carbon atoms on the nanotube surface to their sp^3-hybridized analogues. That is, upon covalent sidewall functionalization, for example, the periodicity of the 1-D lattice can be disrupted by the introduction of defect sites. This may cause destruction of the nanotube band structure, accompanied by a loss of intrinsic so-called van Hove transitions[38,40,67] in the UV-visible-NIR spectra. Oxidative pre-treatment of CNTs tends to be associated with strong acid oxidation and other harsh chemical reactions, which may also unavoidably and invariably disrupt the intrinsic electronic structure of CNTs. In the context of potential applications of CNT–nanoparticle hybrid materials, of particular significance has been the inclination to incorporate these novel building blocks as components of photovoltaic nanodevices. This practical consideration has been a key motivator for developing non-covalent methodologies to rationally and reproducibly functionalize CNTs without destroying their intrinsically favorable optoelectronic properties. Moreover, the utilization of oxidized CNTs may lead to a nonuniform coverage of nanoparticles on the surface as particles tend to attach at the ends and defect sides of carbon nanotubes, where the concentration of carboxylic acid groups is the largest. To this end, the reliable synthesis of CNT–nanoparticle heterostructures *via* non-covalent approaches has attracted a good deal of experimental effort.

2.2.1 Electrostatic interactions. Polymer-wrapping techniques, including the coating of polyelectrolyte shells on the CNT surface, have become one of the more common approaches used to functionalize CNTs through non-covalent attachment of macromolecules. For example, the fluorescence visualization of CNTs in aqueous solutions can be achieved[68] by decorating CNTs with CdSe–ZnS nanocrystals in the presence of sodium dodecyl sulfonate (SDS) surfactant with the semiconducting quantum dots arranging themselves on the sidewalls of SWNTs by virtue of electrostatic interactions between zinc ions in the outer shell and electronegative oxygen atoms associated with the sulfonate group of the surfactant (Fig. 2).

Polyelectrolytes are particularly rich in different terminal functionalities. Hence, by choosing different types of polyelectrolytes, the surfaces of carbon nanotubes can be tailored to be either negatively or positively charged. Consequently, either nanoparticles or nanocrystals of opposite charge can be anchored *via* electrostatic interactions. Additionally, the thickness of these polymeric layers can be controlled by judicious

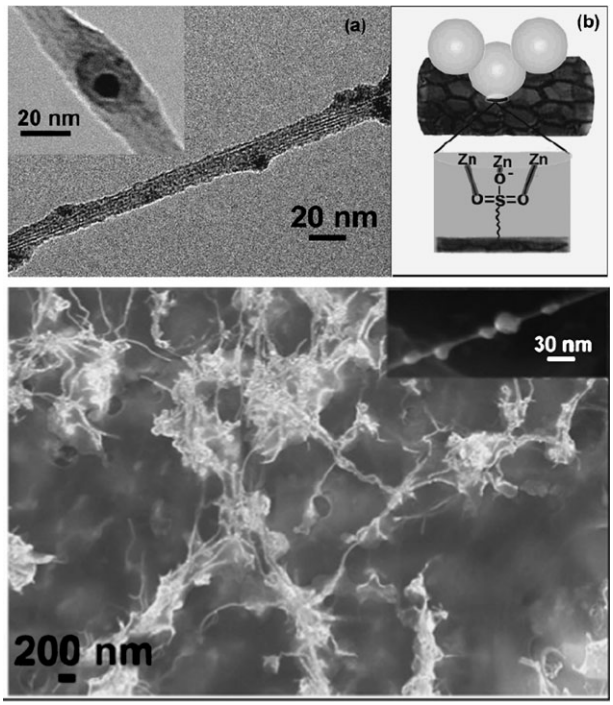

Fig. 2 (Top) (a) Transmission electron micrograph of quantum dots (QDs) attached to the sidewall of a typical SWNT-rope. Inset shows a higher magnification image of a single QD on the surface of an SDS-coated SWNT rope. (b) Schematic illustration of the coordination between the QDs and SWNTs. The electrostatic coordination between dangling Zn ions and O is shown using black-stroked-with-red line. (Bottom) Scanning electron micrograph of SWNT–QD. QD clusters can easily be seen in the close proximity of SWNTs, indicating the labeling procedure. Inset shows the high magnification image of a small SWNT-rope or possibly an individual SWNT. QDs can be clearly spotted on the sidewall. Reprinted with permission from S. Chaudhary, J. H. Kim, K. V. Singh and M. Ozkan, *Nano Lett.*, 2004, **4**, 2415. Copyright 2004, American Chemical Society.

choice not only of the polyelectrolyte itself but also of assembly conditions including pH values and ionic strength parameters. Moreover, these grafted CNT hybrids often demonstrate increased dispersability in useful solvents such as water. Therefore, the presence of noncovalently bound multilayer polyelectrolyte shells on the CNT scaffold offers essentially unlimited opportunities for the subsequent incorporation of a wide variety of different functionalities (including biological molecules and specialty ligands) onto the CNT surface, and hence, the possibility of generating complex, hybrid architectures. For instance, CNT–nanoparticle nanoassemblies can be constructed on the basis of a electrostatic layer-by-layer (LbL) self-assembly technique, which is applicable for many different classes of nanoparticles, such as metallic Pt nanoparticles.[69–71]

For example, Jiang *et al.*[69] achieved the homogeneous distribution of gold nanoparticles onto nitrogen-doped carbon nanotubes which were treated with H_2SO_4–HNO_3 and modified with a cationic polyelectrolyte. The negatively charged gold nanoparticles were attracted by electrostatic interaction to the positively charged polymer chains attached to the carboxylated nanotubes. TEM studies showed that in

Published on 13 February 2009. Downloaded by Pennsylvania State University on 12/09/2016 18:00:11.

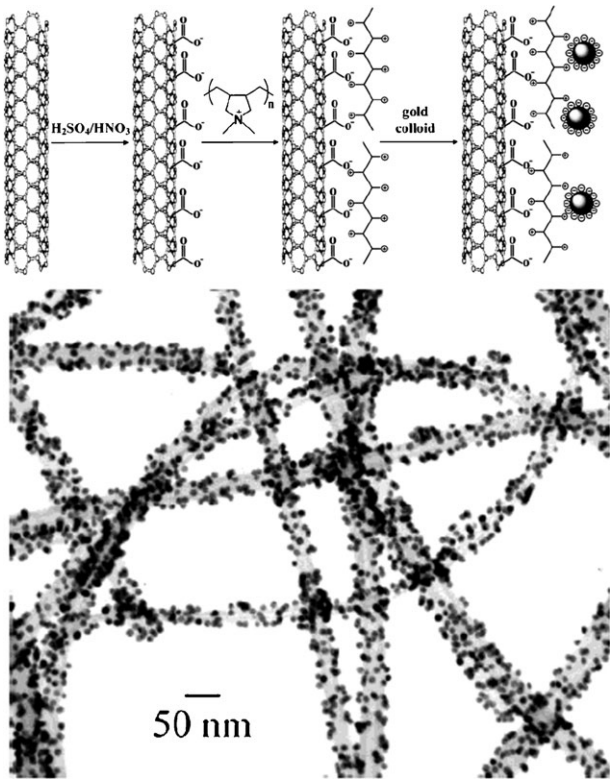

Fig. 3 (Top) Schematic view of the process for anchoring gold nanoparticles to CN_x nanotubes. (Bottom) TEM photograph of gold nanoparticle–CN_x nanotube hybrid structures. Reprinted with permission from K. Y. Jiang, A. Eitan, L. S. Schadler, P. M. Ajayan, R. W. Siegel, N. Grobert, M. Mayne, M. Reyes-Reyes, H. Terrones and M. Terrones, *Nano Lett.*, 2003, **3**, 275. Copyright 2003, American Chemical Society.

the resulting structure, gold nanoparticles were uniformly well-dispersed along the sidewalls and ends of the CNTs (Fig. 3). Conversely, in a similar experiment, Kim *et al.*[72] prepared MWNT–gold nanoparticle composites by adsorbing positively charged gold nanoparticles onto negatively charged MWNTs that had been previously functionalized with anionic polyelectrolytes. A similar electrostatic approach using poly(amphiphiles) has also been used to create Au–CNT composites, composed of polyelectrolytic multilayered films.[73] Specifically, hydrolyzed poly(styrene-*alt*-maleic anhydride) (PSMA) was adsorbed noncovalently onto the surface of carbon nanotubes *via* a hydrophobic interaction. A second polymer, namely polyethyleneimine (PEI), was subsequently covalently attached to the PSMA, forming a cross-linked polymer bilayer. Steps were repeated to create a multilayered film composed of alternating layers of polyanions and polycations that could then be used to mediate the robust attachment of gold nanoparticles.

Several studies have shown that CNTs have a potential application in the fabrication of electrochemical sensors due to the unique potential of CNTs in electron transfer processes. For example, the combination of 2–3 nm Pt nanoparticles and CNTs possesses remarkably improved sensitivity towards hydrogen peroxide, as compared with their bulk analogues, with response times and detection limits in the range of 3 s and 0.5 μM, respectively, with a good linear range over several orders of magnitude of concentration.[74] Very recently, Liu *et al.*[75] fabricated a novel multilayer gold nanoparticle/MWNT/glucose oxidase membrane by electrostatic assembly using positively charged poly(dimethyldiallylammonium chloride) to construct this architecture layer-by-layer. This novel membrane showed excellent analytical performance in the detection of glucose up to 9.0 mM with a detection limit of 128 μM at a relatively low potential (−0.2 V).

In addition, the decoration of CNTs with magnetite nanoparticles *via* electrostatic interaction has been achieved by Jérôme and his coworkers.[71] In the first step, MWNTs were covered with preformed carboxylate-terminated poly-2-vinylpyridine chains by chemical grafting, resulting in a negatively charged surface and hence, a stable dispersibility in water. Subsequent addition of positively charged Fe_3O_4 nanocrystals with an average diameter of 5 nm resulted in MWNTs densely covered with magnetic nanoparticles and responsive to a magnetic field of 1 T. Magnetically coated CNTs, for example, possess intriguing promise as tips for use in high-resolution magnetic force microscopy (MFM). Electrostatic self-assembly has also been utilized to load MWNTs with CdTe quantum dots as well as with Fe_3O_4 magnetic nanoparticles.[76]

The Giersig group[77] carried out a series of experiments on the fabrication of CNT–nanoparticle composites by employing polymer wrapping and LbL techniques. They wrapped their MWNTs with poly(allylamine hydrochloride) (PAH), which was noncovalently adsorbed onto the MWNT surface as a result of van der Waals interactions and mechanical anchoring. Subsequently, 10 nm-sized ZnO,[78] CdSe,[78] and CdSe–CdS[78] nanocrystals were attached to the polymer layer through interaction with amine groups of PAH, thereby ensuring good separation and stability in aqueous solution due to electrostatic interactions. TEM studies suggested that the attached particles on the CNT surface were homogeneous in size, shape and distribution with no obvious clustering. Moreover, since the MWNT–PAH system was stable in either polar or nonpolar solvents, hybrid materials could be flexibly generated from a variety of either aqueous or organic dispersions of nanocrystals.

The same group also demonstrated that the presence of a silica coating on the MWNTs could preserve the intrinsic luminescence features of the attached quantum dots by preventing either charge or electron transfer between the MWNTs and the quantum dots themselves. This observation was consistent with a similar work, which involved both tuning the optical properties and minimizing the photoluminescence quenching of CdTe–silica–CNT nanocomposites by employing polymer wrapping and LbL techniques.[79] MWNTs were first wrapped with polystyrene sulfonate (PSS) possessing negatively charged sulfonate groups, followed by the homogeneous adsorption of the cationic polyelectrolyte, poly(diallyldimethylammonium chloride) (PDDA). Subsequent assembly of negatively charged CdTe nanocrystals, capped with thioglycolic acid, onto the PSS/PDDA-coated CNT constructs was driven by electrostatic interactions. Photoluminescence quenching could then be controlled through the growth of a silica shell onto the CNTs prior to LbL assembly, thereby isolating the CdTe nanocrystals from

 This journal is © The Royal Society of Chemistry 2009

Published on 13 February 2009. Downloaded by Pennsylvania State University on 12/09/2016 18:00:11.

the CNTs. It was proposed that the large band gap and thickness of the SiO_2 layer could screen the background nanotube absorption and thereby prevent both charge transfer and electron tunneling that would have resulted in unfavorable photoluminescence quenching. In essence, the energy levels of the CdTe remained unaffected, thereby preserving quantum confinement effects.

Using a similar technique, linear assemblies of silica-coated gold nanoparticles on carbon nanotubes could also be obtained.[80] The addition of salt could dramatically increase the thickness of the polymeric PSS/PDDA layer on the MWNTs with lengths of up to 8 microns. The presence of the silica layer could avoid particle aggregation. Moreover, a shift of the plasmon band, *i.e.* a tailoring of optical properties, of the silica-coated gold nanoparticles was observed upon alteration of the thickness of the outer silica layer. That is, UV-visible spectroscopy studies showed that the band for the nanocomposites was red-shifted with respect to that of the corresponding nanoparticles, due to interparticle interactions. The same group also aligned gold nanorods onto carbon nanotube surfaces,[81] using the same approach, with the Au serving as a label to monitor the degree of alignment of the nanotubes within the polymer film.

2.2.2 Hydrophobic interactions. To avoid potentially complicated and tedious surface modification of CNTs, groups have taken advantage of hydrophobic interactions between appropriately functionalized nanoparticles and pristine CNTs to develop simple and effective strategies for assembling CNT–nanoparticle nanocomposites. In some cases, non-specific, physical mixing of dispersions of both CNTs and nanoparticles has been sufficient to effectively prepare CNT–nanoparticle nanocomposites.[82]

For example, the Zhong group[83,84] was able to fabricate a very stable assembly of alkanethiolate-capped gold nanoparticles with 2–5 nm core sizes onto CNTs through a combination of hydrophobic and hydrogen-bonding interactions between the alkyl capping shell of the nanoparticles and the hydrophobic surface of the CNTs (Fig. 4, top). TEM was used to detect the presence of densely packed gold particles with controllable coverage on the CNT surface. They also claimed that the particle size, shape, dispersion and relative concentrations of nanoparticles used could be utilized to controllably alter the morphology and packing density for nanoparticles assembled on the CNT surface (Fig. 4, bottom). It was also experimentally and theoretically demonstrated that the coverage of gold nanoparticles at the surface of alkyl- and alkylthiol-modified MWNTs decreased as a function of increasing alkyl chain length, due to steric issues, associated with chain movement.[85] Furthermore, acetone molecules adsorbed on CNTs have also been used to anchor octanethiol capped Au nanoparticles measuring 1–3 nm diameter onto carbon nanotube sidewalls.[86] A related example[87] involves the specific interaction between Au nanoparticles and the nitrogen atoms of bamboo-like carbon nanotubes (BCNTs), produced by pyrolysis of iron(II) phthalocyanine at 950 °C, coupled with the hydrophobic interaction between the alkyl chains of the capping molecules and the hydrophobic backbones of the nanotubes themselves. The spatial distribution of Au

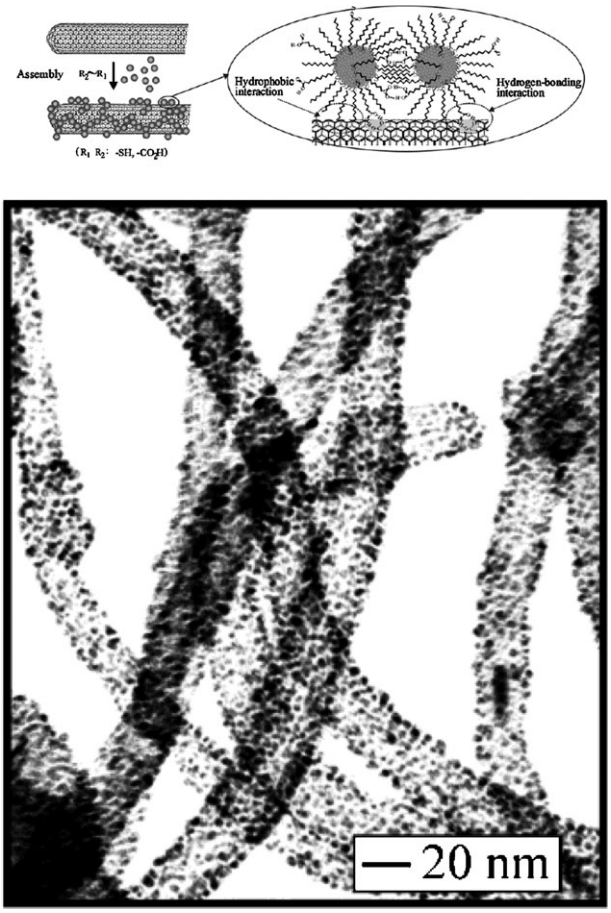

Fig. 4 (Top) Schematic illustration of the molecularly mediated assembly of monolayer-capped nanoparticles onto a CNT. (Bottom) TEM micrographs for NDT–Au_{2nm}/CNTs derived under different assembly conditions: (a) [NDT] = 3.1 mM, [Au_{2nm}] = 6.3 μM, and 0.27 mg of CNTs mL^{-1} (NDT = 1,9-nonanedithiol). Reprinted with permission from L. Han, W. Wu, F. L. Kirk, J. Luo, M. M. Maye, N. N. Kariuki, Y. H. Lin, C. M. Wang and C. J. Zhong, *Langmuir*, 2004, **20**, 6019. Copyright 2004, American Chemical Society.

nanoparticles with an average size of 3.9 nm was noted to be quite uniform with a high density noted on both the sidewall and tips of BCNTs, attributable to the presence of nitrogen atoms on the BCNTs and related Au–N interactions. The reaction was found to be efficient and facile enough that only hand shaking for 1 min was required for its synthesis.

In terms of related experiments,[88] it was found that gold nanowires can be self-assembled from the fusion of discrete Au nanocrystals grown on the backbone of a carbon nanotube by mixing CNTs with a dispersion of tetraoctylammonium bromide modified gold nanoparticles, measuring 6 nm in diameter. It was suggested that the driving force for the self-assembly process was associated with charge transfer from the conduction band states of the gold nanoparticle to the continuum of π* states of the carbon nanotubes themselves. Later, Sainsbury *et al.*[89] reported the use of phosphonic acid-modified and alkoxysilane-modified MWNTs to template the assembly of semiconducting and insulating particles such as titanium dioxide and silica nanoparticles.[90] The resulting hybrid materials provided the potential basis for the use of

Published on 13 February 2009. Downloaded by Pennsylvania State University on 12/09/2016 18:00:11.

these structures as building blocks for sensors, nanoscale switches, as well as other devices.

2.2.3 π–π Stacking interactions. A π–π interaction can be considered as an electrostatic interaction between aromatic species possessing π-electron rich structures and the highly delocalized π-electron cloud surrounding the CNT surface. Such interactions with CNTs can be surprisingly strong, capable of withstanding temperatures of >400 °C.[91] Not surprisingly, molecules, containing conjugated π aromatic structures, such as pyrene, porphyrins and thionine,[92] have been used as linkers with which to anchor a range of nanoparticles (as diverse as Pt, CdS and silica)[93] onto CNT surfaces.

It has been reported that while thiol-terminated[94] or amino-terminated[95] pyrene can bind to gold nanoparticles through either the thiol or amine linkage, the pyrene chromophore itself can be noncovalently attached to the sidewall of a carbon nanotube *via* π–π stacking interactions. Spectroscopic experiments have suggested that in these systems, the linker pyrene's fluorescence was largely quenched due to charge transfer between the CNTs and Au nanoparticles. Based on the same principle, magnetic nanoparticles can be adsorbed onto CNTs using a carboxylic acid derivative of pyrene as an intermediary linker, resulting in magnetic modification of the carbon nanotube surface.[96] Moreover, such nanotube composites, containing pyrene, are quite soluble in organic solvents as compared with pristine nanotubes. Guldi *et al.*[97] have prepared CNT–CdTe nanohybrids (Fig. 5) by modifying CNTs with pyrene. Spectroscopic studies of the composite material showed that the optical properties of CdTe were affected due to a charge-transfer interaction between the photoexcited electron donor (*e.g.* CdTe) and the electron acceptor (*e.g.* CNTs). A relatively high incident photon-to-charge carrier generation efficiency (IPCE) value of up to 2.3% was achieved for hybrid cells consisting of single SWNT/pyrene/red-emitting CdTe stacks.

Similarly, Pt nanoparticles have been immobilized onto benzyl mercaptan-modified MWNTs through the formation of strong Pt–S bonds, as demonstrated by Pt 4f and S 2p XPS spectra.[91] Specifically, in the case of benzyl thiol, the phenyl ring participates in π–π interaction with the walls of the CNT, and the small dimension of the phenyl ring itself permits a high density of thiol groups onto the CNT surface as well as a shorter electrical contact distance between the Pt nanoparticle and the CNT. All of these factors led to a correspondingly high density of Pt nanoparticles in the product conjugate. Similarly, under ambient conditions and in the absence of acid,[98] a high density of well-dispersed Pt nanoparticles, modified with the organic molecule, triphenylphosphine, was successfully loaded onto MWNTs without pretreatment. These nanotube conjugates evinced higher electrocatalytic activities as compared with commercial catalysts. The sizes of the Pt nanoparticles were noted to be somewhat smaller than 4 nm and the content of Pt could be reliably varied from 3.1 to 40.6 wt% by manipulating the relative concentrations of CNTs and metal nanoparticles.

2.2.4 Summary of non-covalent approaches. The attractiveness of the noncovalent approach is fundamentally related to its inherent experimental facility and simplicity. Moreover, this type of structurally non-destructive carbon nanotube functionalization allows for the preservation of the intrinsically interesting optoelectronic properties (such as van Hove transitions) of these materials. In addition, unlike with covalent functionalization, the non-specificity of noncovalent functionalization renders it possible to uniformly coat nanotubes with a relatively high density of nanocrystals. In addition, it is also likely that the electrostatic interactions used to create some of these assemblies are reversible and hence tunable, upon slight changes in the local charge environment, as induced by alterations in ionic strength and pH.

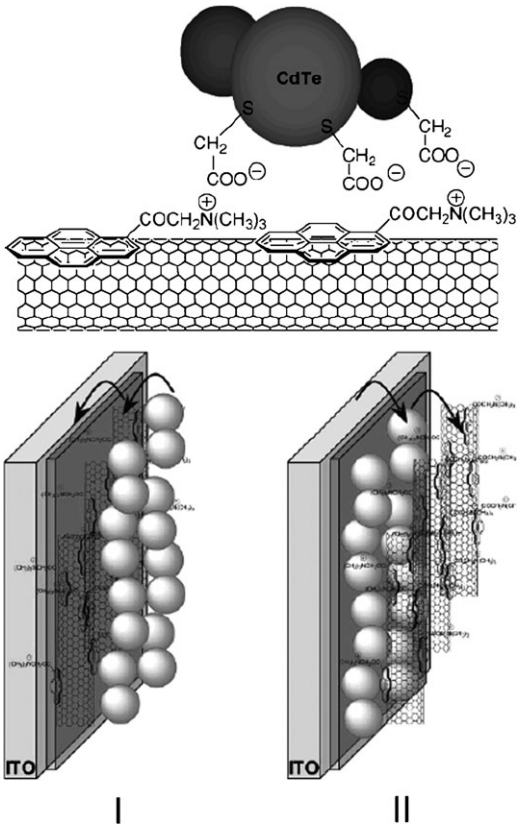

Fig. 5 (Top) Partial structure of the SWNT/Pyrene$^+$/CdTe described in this work. (Bottom) Cartoon that exemplifies the Working Mode of CNT/Pyrene$^+$/Red CdTe (I) and Red CdTe/CNT/ Pyrene$^+$ (II) Hybrid Cells. Reprinted with permission from D. M. Guldi, G. M. A. Rahman, V. Sgobba, N. A. Kotov, D. Bonifazi and M. Prato, *J. Am. Chem. Soc.*, 2006, **128**, 2315. Copyright 2006, American Chemical Society.

2.3 Direct formation of NPs on CNTs

Although a coating of pre-synthesized nanoparticles on the CNT surface can be realized through either covalent or non-covalent interactions including electrostatic interactions, hydrophobic interactions, and π–π stacking interactions, the presence of the organic protecting shell may interfere with the functions of metal nanoparticles. For instance, the presence of such a dielectric shell layer may degrade favorable properties such as electrical conductivity, which, in turn, would impair electrocatalytic performance. In addition, the introduction of extra linker molecules may imply a more tedious experimental

 This journal is © The Royal Society of Chemistry 2009

Published on 13 February 2009. Downloaded by Pennsylvania State University on 12/09/2016 18:00:11.

procedure and associated higher costs. To this end, direct formation of nanoparticles onto the CNT surface has become a reasonably attractive goal. A generalized protocol to form either nanoparticles or nanocrystals directly onto the carbon nanotube surface has been to functionalize the external walls of nanotubes first through a chemical reaction, such as through the use of either strong acids, ultrasonication, or microwave irradiation, followed by deposition of metal particles onto the functionalized nanotube sidewall surface *via in situ* growth, chemical reduction, or electrodeposition reactions.

2.3.1 *In situ* growth without the presence of reducing agents. *In situ* growth involves a facile one-pot synthesis method widely used for either nanoparticles or nanocrystals without the need for any additional reducing agent or irradiation treatment. Carboxylic acid functional groups, introduced onto the surfaces of CNTs by means of oxidative chemical treatment, can therefore not only enhance the solubility of CNTs but also assist in their coordinative complexation with metal ions, thereby giving rise to preferred sites of nucleation on the nanotube surface.

In 2002, the Dai group[99] reported that for certain metal salt solutions such as Na_2PtCl_4 and $HAuCl_4$, metal deposition essentially occurred spontaneously after simple immersion of the CNTs in the appropriate metal salt solution for a few minutes, presumably due to a direct redox reaction between the metal ions and the SWNTs themselves. Based on a similar principle, Kong *et al.*[100] fabricated SWNT/gold nanohybrids by simply immersing the SWNT film in a gold salt solution. Monodisperse, spherical gold nanoparticles with a mean diameter of 25 nm were formed after immersion and a reaction time of 10 min. The deposition of these Au nanoparticles significantly enhanced the conductivity of the SWNT film (to a maximum of 2×10^5 S m^{-1}) without a substantial change in their transmittance of visible light, with potential implications for their utilization as transparent conductive electrodes in touch screens, large-area flexible displays, flexible solar panels, and thin film transistors.

This electroless deposition process, with respect to electrodeposition itself, is limited by the fact that only metal ions of a redox potential higher than that of a reducing agent or carbon nanotube can be transformed into nanoparticles on the nanotube support. Consequently, Cu^{2+} and Ag^{+} cannot be reduced into metal nanoparticles due to their lower redox potentials. Therefore, Qu and Dai exploited[101] a process known as 'Substrate-Enhanced Electroless Deposition (SEED)', described in Fig. 6, to enable the electroless deposition of a large variety of metal nanoparticles on the CNT surface in the absence of any additional reducing agent. In essence, by supporting CNTs with a metal substrate of a redox potential lower than that of the metal ions to be reduced into nanoparticles, it was determined that metal ions even with a redox potential lower than that of a CNT could be readily reduced into metal nanoparticles onto the nanotube support. For example, by immersing Cu-supported MWNTs into an aqueous solution of $HAuCl_4$, Au clusters with an average diameter of around 100 nm were found to deposit along the nanotube sidewalls after about 10 s of reaction. Ag, Cu, Pt and

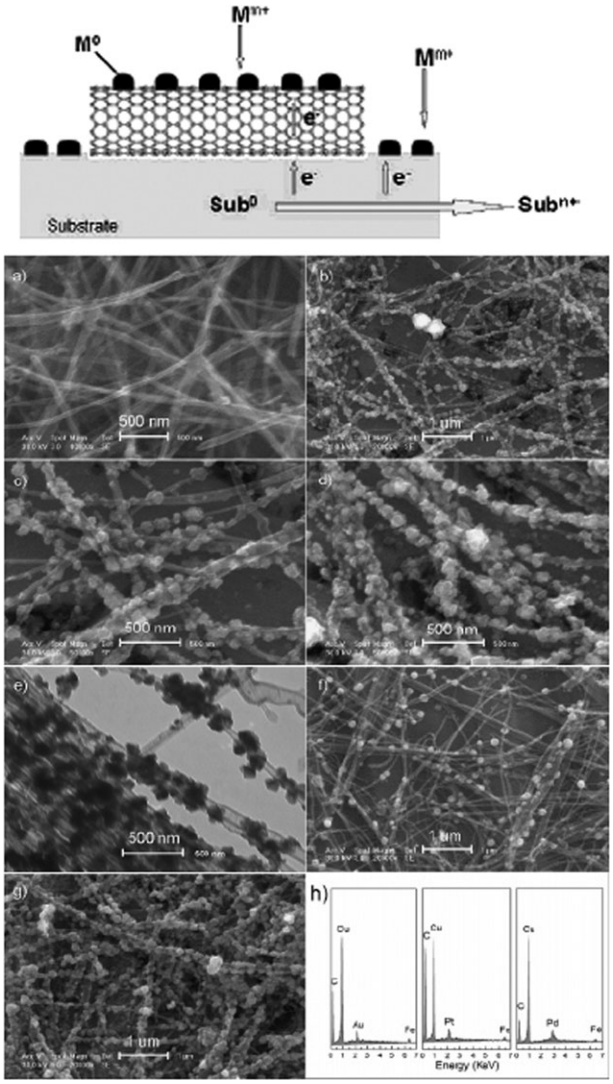

Fig. 6 (Top) Schematic illustration of metal nanoparticle deposition on carbon nanotubes *via* the SEED process. (Bottom) SEM images of MWNTs supported by a copper foil after being immersed into an aqueous solution of $HAuCl_4$ (3.8 mM) for different periods of time: (a) 0 s, (b) 10 s, (c) same as for (b) under a higher magnification, (d) 30 s. (e) A transmission electron microscopic (TEM) image of Au nanoparticle-coated MWNTs, (f) the Cu-supported MWNTs after being immersed into an aqueous solutions of K_2PtCl_4 (4.8 mM) for 10 s, and (g) the Cu-supported MWNTs after being immersed into an aqueous solution of $(NH_4)_2PdCl_4$ (7.0 mM) for 10 s. (h) EDX spectra for the Au, Pt, and Pd nanoparticle-coated MWNTs on Cu foils. Reprinted with permission from L. T. Qu and L. M. Dai, *J. Am. Chem. Soc.*, 2005, **127**, 10806. Copyright 2005, American Chemical Society.

Pd nanoparticle-coated SWNTs could also be similarly prepared using the same process. By employing the SEED technique, Qu *et al.*[102] achieved size (*i.e.* 100 to 500 nm) and shape (*i.e.* cube *vs.* sphere) control of Pt and Au nanoparticles for site-selective (*i.e.* outer wall, inner wall, or end tip) modification of carbon nanotubes. These CNT-supported metal nanoparticles were found to possess interesting optical and electrocatalytic properties.

Transition metal nanoparticles, such as Ru, Cu, Zn and Sn, have been noted to spontaneously form onto

Published on 13 February 2009. Downloaded by Pennsylvania State University on 12/09/2016 18:00:11.

2,2′: 6,2″-terpyridine (Terpy) modified SWNTs.[103] To generate these systems, SWNTs were initially modified with Terpy by simply immersing SWNTs in a Terpy solution for 1 h at room temperature. It was suggested that the origin of the electronic coupling involving Terpy was related to an interaction between nonbonding electrons of the three nitrogen atoms in Terpy and the π electrons of the SWNTs. The main driving force for the subsequent formation of nanoparticles was thought to be electron transfer from the Terpy–SWNTs to the transition metal ions. Elevation of the Fermi level of the SWNTs occurred due to electrons injected from Terpy into the SWNTs, thereby enabling spontaneous electron transfer.

Furthermore, in the presence of carboxyl group-functionalized or poly(acrylic acid) (PAA) grafted CNTs, silver nanoparticles could be generated *in situ* from an aqueous solution of $AgNO_3$ at room temperature, leading to the formation of CNT/Ag nanohybrids.[104] Silver nanoparticles could be controlled from a size of 2 to 20 nm with loading levels as high as 82%. By comparison, a high loading of almost monodisperse Pt nanoparticles on SWNT was achieved by mixing sodium dodecylbenzene sulfonate (SDBS)-assisted solubilized SWNTs with Pt carbonyl complexes.[105] As-obtained Pt nanoparticles with an average diameter of 2.2 nm were broadly dispersed, even at a 60 wt% loading. The high-surface-area nanoparticle–SWNT conjugates exhibited enhanced electrocatalytic activity for methanol oxidation. Moreover, Ag, Cu, Au and Pt nanoparticles of tunable sizes up to 11 nm have been grown and anchored *in situ* onto MWNTs modified with fourth-generation NH_2-terminated poly(amido amine) dendrimers.[106]

Of the various classes of nanoparticles prepared, semiconducting metal chalcogenide nanocrystals have been the most intensively studied due to their quantum confinement effects as well as to size-and shape-dependent photoemission characteristics. Recently, the *in situ* growth of different types of metal chalcogenide nanocrystals, such as CdSe,[107] CdTe,[35,108] CdS,[41,109] ZnS,[110] PbS,[111] and Cu_2S,[31] on CNT surfaces has been reported.

One of these initial studies[107] reported on the use of ozonized[40,112] SWNTs as ligands for the controlled growth of CdSe quantum dots. Specifically, CNTs were used as templates for the subsequent formation of quantum dots. It was proposed that carboxylic groups, introduced by treating CNTs with ozone, could cover up to 30% of the external surface area of the tubes and act as reactive sites with which to coordinate organometallic metal precursors, leading to the rational formation of CdSe quantum dots. By comparing results of the growth of the quantum dots using variously oxidized nanotube templates, it was suggested that the degree of immobilization (and hence, corresponding density) of the resulting CdSe on the nanotube surface readily correlated with the degree of oxidation. Furthermore, based on the same protocol (Fig. 7), analogous CdTe–MWNT[108] and CdTe–SWNT[35,113] hybrid materials could also be generated.

More interestingly, it has recently been found that the presence of CNTs can trigger a morphological transformation of CdSe nanorods into tightly bound pyramidal-shaped nanoparticles. This nanotube–nanoparticle interaction can be understood as a consequence of ligand exchange. The

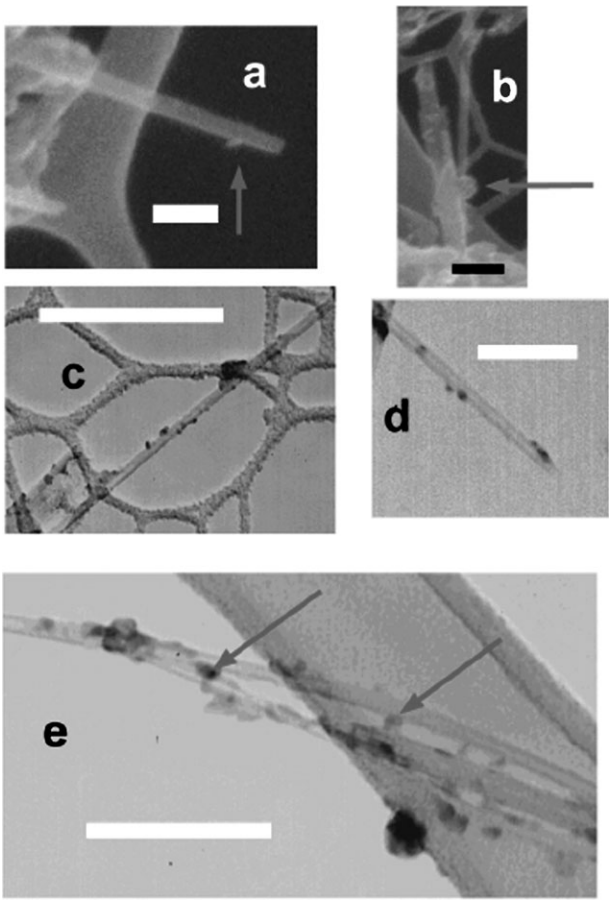

Fig. 7 (a) Scanning electron micrograph (SEM) of a particle grown near the tip of the tube. (b) SEM image of a nanocrystal-mediated junction with carbon nanotube bundles. Arrows point to CdTe. Scale bars for SEM images are 100 and 200 nm, respectively. The presence of CdTe was confirmed by EDS signals for Cd and Te. Parts (c)–(e) show transmission electron microscopy images. (c) Sidewall coverage of quantum dots on a MWNT bundle. (d) CdTe nanocrystals on nanotube sidewalls, with some near the tip edge. (e) Nanocrystal-mediated nanotube junctions indicated by arrows. Scale bars for TEM images are 180, 75 and 112 nm, respectively. Reprinted with permission from S. Banerjee and S. S. Wong, *J. Am. Chem. Soc.*, 2003, **125**, 10342. Copyright 2003, American Chemical Society.

released ligands (*i.e.* octadecylphosphonic acid (ODPA)) promote the transformation of CdSe nanoparticles by selective etching and classic Ostwald ripening,[114] as shown in Fig. 8. In another case, the size and morphology of Cu_2S nanocrystals on a MWNT surface depended strongly on the concentration of precursors used. For instance, when the concentration of $Cu(acac)_2$ was below 0.1 M, spherical Cu_2S nanoparticles with 4 nm were obtained, whereas at concentrations higher than 0.15 M, the nanoparticles, with an average size of 12 nm, assumed a triangular morphology, as confirmed by TEM and HRTEM images.[31] In any event, MWNTs directly attached to the Cu_2S nanocrystals could facilitate the generation of a photocurrent by trapping the conduction band electrons, a process resulting in charge separation and retardation of the recombination process.

Kamat *et al.*[109] developed a simple and convenient method for preparing SWNT–CdS composites by initially using the

 This journal is © The Royal Society of Chemistry 2009

Published on 13 February 2009. Downloaded by Pennsylvania State University on 12/09/2016 18:00:11.

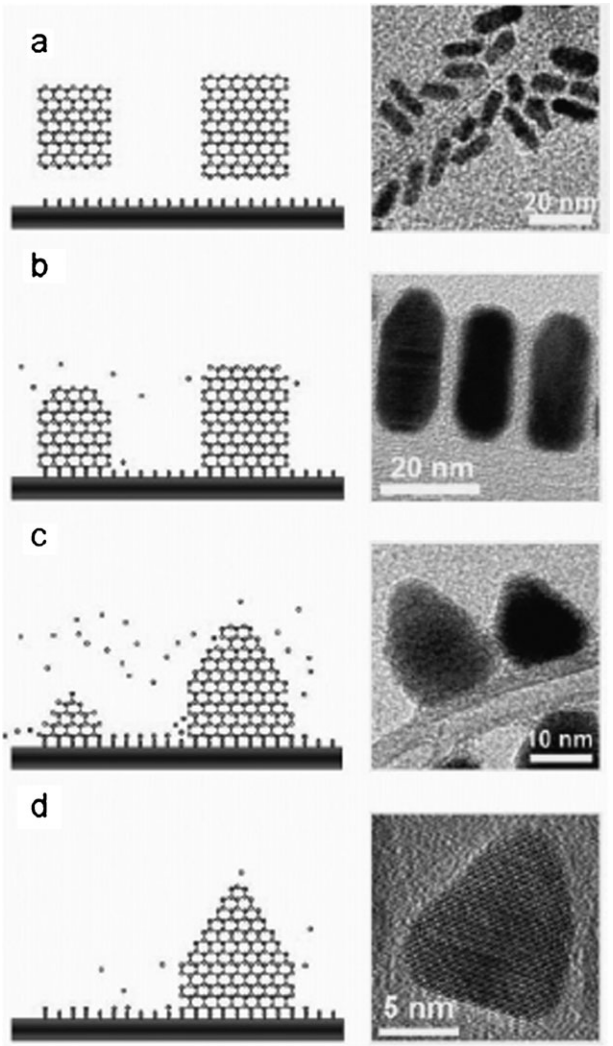

Fig. 8 Proposed mechanism for the interaction and morphological transformation of CdSe nanorods in the presence of CNTs (with corresponding TEM example images). (a) nanoparticle-CNTs interaction, (b and c) selective etching, (c and d) selective etching and Ostwald ripening, (d) final shape of the pyramidal nanoparticles. Reprinted with permission from B. H. Juarez, C. Klinke, A. Kornowski and H. Weller, *Nano Lett.*, 2007, **7**, 3564. Copyright 2007, American Chemical Society.

hydrophobic chains of the tetraoctylammonium bromide (TOAB) surfactant, which rendered SWNTs soluble in THF; these functionalized nanotubes were then complexed with Cd^{2+} ions, thereby allowing for conversion to CdS upon reaction with S^{2-}. The diameter of the as-prepared CdS nanoparticles thereby grown on the surface of SWNTs measured from 6–9 nm. Transient absorption spectroscopy yielded a rate of 4×10^8 s^{-1} for electron transfer between excited CdS and the SWNTs. Such composite films showed potential as building blocks for light-harvesting arrays and additional optoelectronics applications. Recently, Gu *et al.*[115] reported a facile route for the large-scale synthesis of uniform ZnS-coated carbon nanotubes based on a solution-chemical approach. The thickness of the ZnS shell could be tuned from 12 to 25 nm by rationally varying the amount of reagents as well as reaction time.

CNT/oxide hybrids have also been synthesized by using an *in situ* growth method. Examples include TiO_2,[108,116] Fe_3O_4, ZnO,[117,118] and SnO_2.[119] For instance, anatase TiO_2 nanoparticles with a size range of 2 to 10 nm have been formed on polyethyleneimine (PEI) coated carbon nanotubes by controlled hydrolysis of titanium bis-ammonium lactato dihydroxide (TALH) in the presence of urea.[116] Anatase TiO_2 nanoparticles (18.5, 8.5 and 6.3 nm)[120] were grown on MWNTs using the sol-gel method, while rutile TiO_2 nanorods, with a diameter range of 20–60 nm and a length distribution of 50 to 150 nm, have been uniformly deposited on MWNTs using the hydrothermal method. ZnO has been grown onto MWNT templates through a thermal decomposition reaction involving $Zn(NH_3)_4CO_3$ and polyvinyl pyrrolidone (PVP) polymer.[117] Crystalline, monodisperse ZnO nanoparticles have also been fabricated onto MWNT surfaces at low temperature by mixing a $Zn(NO_3)_2{\cdot}4H_2O$ precursor with nitric acid-treated MWNTs.[118] Using the same principle,[119] SnO_2 nanoparticles possessing a diameter range between 1 and 6 nm can be cast as a thin uniform layer onto a SWNT surface by using anhydrous $SnCl_2$ as a precursor in the presence of nitric acid-treated SWNTs at room temperature.

2.3.2 Chemical reduction deposition. Such a protocol involves the adsorption of a metal salt onto the CNT surface followed by reduction of the metal salt in the presence of reducing agents, such as (i) an atmosphere of H_2[121,122] at high temperature,[123,124] as well as (b) conventional reagents such as $NaBH_4$,[125–127] citric acid,[128] and ethylene glycol.[12,122] In this regard, a large number of different types of nanoparticles have been attached onto the nanotube template.

For instance, Chen *et al.*[129] developed a controllable way of synthesizing Cu nanoparticles by adding a desired amount of a Cu salt to the CNT dispersion followed by precursor decomposition under H_2 at temperatures below 773 K. Results showed that the diameter of the as-prepared Cu nanoparticles correlated with the diameter of the CNTs, the ratio of the amount of Cu salt to that of the CNTs, as well as the precursor decomposition temperature. Furthermore, the same group extended this method to facilitate the production of several commonly used metal nanoparticles, such as Pd, Pt, Ag and Au nanoparticles with average sizes of 7, 8, 8 and 17 nm, respectively, onto nanotube surfaces. However, in those cases, the observed size distribution increased from <5 nm to greater than tens of nanometers.[121]

With respect to transition metal nanoparticles in particular, Lin *et al.* deposited Pd, Ru and Rh nanoparticles onto functionalized MWNTs through a simple hydrogen reduction of metal–β-diketone precursors under supercritical carbon dioxide conditions.[124] It should be noted that different groups discovered that even the use of $PdCl_2$ or $RuCl_3{\cdot}3H_2O$ was sufficient as the metallic precursor in either supercritical carbon dioxide[130] or supercritical water[131] to accomplish similar types of reactions. Later, based on the same principle, Pt nanoparticles[123] were also obtained using platinum(II) acetylacetonate as the metallic precursor. In addition, Yu *et al.*[122] investigated the degree of deposition of Pt clusters on CNT surfaces, prepared under different oxidative treatments. Their results suggested that the H_2SO_4–HNO_3

Published on 13 February 2009. Downloaded by Pennsylvania State University on 12/09/2016 18:00:11.

treatment, in particular, yielded a large and well-dispersed density of Pt nanoparticles due to a higher concentration of carboxyl, carbonyl, phenolic and sulfate groups introduced onto the surface of CNTs, available for metal ion coordination and particle nucleation. Furthermore, Giordano *et al.*[132] decomposed the dimeric complex $[Rh_2Cl_2(CO)_4]$, which had been grafted onto carboxylate-terminated MWNTs, under dihydrogen conditions at 573 K so as to obtain highly dispersed rhodium nanoparticles with a diameter range of around 1.5–2.5 nm. This novel Rh-supported carbon material was used as a catalyst for the hydrogenation of *trans*-cinnamaldehyde as well as the hydroformylation of hex-1-ene in the liquid phase.

Regarding the formation of noble metal nanoparticles, $NaBH_4$ has remained as a common reducing agent. For instance, Zhang *et al.*[126] were able to generate Au nanoparticles by reducing $HAuCl_4$ in the presence of $NaBH_4$ in solution, and stabilizing the resultant nanoparticles using SDS surfactant. Similarly, the surfactant poly(styrene-*alt*-maleic acid) (PSMA) has been used to disperse SWNTs as well as to bind metal ions onto SWNT surfaces.[127] In particular, it has been suggested that incubation of SWNT–PSMA with metal ions prior to $NaBH_4$ reduction is crucial, as it allows for metal ions to strongly bind onto SWNTs. However, the experimental results of Hu *et al.*[125] indicated that the gold nanoparticles, which had been *in situ* grown onto thiol modified CNTs, were somewhat more polydisperse in size than pre-synthesized gold nanoparticles, which had been self-assembled onto functionalized CNT surfaces. In that case, it was proposed that thiol monolayers, coating the gold nanoparticles during the initial nucleation stage, affected the size of nanoparticles subsequently generated. As a different, supporting example to highlight the role of thiol, Kim *et al.*[133] reduced the Pt precursor $H_2[PtCl_6]$ onto thiolated MWNTs with $NaBH_4$ followed by heat treatment to eliminate the thiol groups. This permitted single Pt atoms to subsequently form Pt clusters upon quenching to room temperature, which could then later grow in size with increasing temperature.

Using citric acid as the reducing agent, Zanella *et al.*[128] focused on the deposition of Au nanoparticles on MWNTs that had been initially derivatized with 1,6-dithiol and 2-aminothiol. A 5.3 wt% Au loading on the 1,6-dithiol MWNT derivative was achieved with an average particle size of 1.7 nm. The higher observed loading of Au on the 1,6-dithiol derivative as compared with the 2-aminothiol derivative (associated with 3 wt% of Au) could potentially be attributable to the fact that each dithiol molecule contains two sulfur atoms (5.3 wt% of S) whereas each aminothiol molecule possesses only one S atom (3.2 wt% of S). Very recently, Zhang *et al.* reported a simple synthesis of MWNT/Au nanocomposites by using a traditional citrate reduction method in the presence of MWNTs.[134] The size of the attached gold nanoparticles was controlled by the amount of added sodium citrate solution. It was shown that MWNTs could be uniformly coated with Au nanoparticles with average sizes of 22 and 12 nm, when 1.5 and 4 ml of sodium citrate solution were respectively added to the mixture.

The "polyol" method, normally used to prepare colloidal suspensions of metal nanoparticles, can be adapted, in the presence of templates such as CNTs, to immobilize deposited nanoparticles. In the absence of CNTs, a typical protocol involves refluxing of a solution of metal salt precursor at 393–443 K in a polyol solvent such as ethylene glycol (EG), where the polyol decomposes to yield the reducing agent needed for metal ion reduction.[135] By extension, one of the first studies[12] reported metal-loaded SWNT material using this technique by encouraging the formation of bonds between Pt and SWNT surfaces through ion exchange with carboxylic acid sites initially created on the nanotube surface by slow wet oxidation in dilute nitric acid. The adsorbed Pt precursors were then reduced by ethylene glycol. In doing so, the group was able to load oxidized SWNTs with 10 wt% of Pt nanoparticles with an average size of 1–2 nm. The role of CNTs in metal-support interactions, related to hydrogenation reactions, was also investigated. Later, Pt–MWNTs were also prepared[136] by the EG method and turned out to possess a high and relatively homogeneous dispersion of spherical Pt nanoparticles with sizes in a range of 2–5 nm. By comparison, Pt nanoparticles have been deposited on MWNTs by HCHO reduction. Studies of the catalytic efficiency of these particular materials in a direct methanol fuel cell (DMFC) indicated that MWNT–supported catalysts prepared by EG reduction were superior to both carbon black XC-72-supported catalysts as well as Pt–SWNT nanocomposites prepared by HCHO reduction, an observation attributed to the greater dispersion of the supported Pt particles. Recently, the "polyol" method[137] was improved through the introduction of suitable amounts of sodium hydrogen sulfite ($NaHSO_3$) and calcium hydroxide aqueous solution as additives to ethylene glycol (EG), thereby forming a modified reducing agent. This protocol gave rise to enhanced formation of a Pt–Ru/CNT composite with high metal deposition efficiency, excellent nanoparticle morphology, and a desirable electrocatalyst composition, with improved catalytic performance for methanol electrooxidation. It should be mentioned that this technique is not limited to the creation of Pt-containing conjugates. For instance, 'tadpole'-like Fe_3O_4–MWNT heterojunctions[138] have been successfully synthesized by positioning Fe_3O_4 spheres onto the tips of MWNTs using a polyol-medium solvothermal method, while MWNTs have been modified[139] with würtzite ZnS nanocrystals in the presence of $ZnCl_2$, thiourea, and EG at 150 °C.

A number of variations on all of these treatments has also been used as means to achieving the same goal. For instance, Au, Pt and Rh nanoparticles were deposited on SWNT surfaces by a mild reduction of metallic salt precursors (such as chlorides or acetylacetonates) using polyethylene glycol (PEG)-200 as a reducing agent. This polymeric functionalization process simultaneously coated the SWNTs with organic molecules such as oleylamine, providing a high degree of solubility for the resulting composites in a number of different organic solvents.[140] Similarly, highly dispersed Pt nanoparticles[141] have been deposited on SWNTs by wrapping the SWNTs in a polymer, such as poly(sodium 4-styrenesulfonate), which breaks up nanotube bundles in order to achieve better dispersion. The size of Pt nanoparticles was 2–3 nm and the loading of Pt nanoparticles onto the nanotube surface achieved levels of up to 30 wt%. The improved catalytic dispersion facilitated diffusion of reactant species which in

 This journal is © The Royal Society of Chemistry 2009

Published on 13 February 2009. Downloaded by Pennsylvania State University on 12/09/2016 18:00:11.

turn resulted in higher methanol oxidation currents and hence more positive potentials for oxygen reduction. Very recently, PEI, which acts as a functionalizing agent for the carbon nanotubes as well as a reducing agent for the formation of Au nanoparticles, has been used to fabricate CNT/Au composites without an extensive surface oxidation process of CNTs.[142] In that experiment, the coverage of Au nanoparticles was tuned by parameters such as the ratio of PEI to $HAuCl_4$ and the relative concentration of PEI and $HAuCl_4$ to MWNTs, as well as the temperature and duration of the heat treatment.

2.3.3 Electrodeposition. Electrodeposition is considered as an attractive technique for the deposition of metal nanoparticles because of the high purity of the resulting metal nanoparticles obtained[143,144] and the relatively easy manipulation of the particle size and distribution by tailoring deposition conditions, such as the applied potential and deposition time. The nanotube in effect acts as a nonsacrificial template for the deposited clusters. Additionally, apart from avoiding potentially complicated treatments required for wet chemical modification of CNTs, electrodeposition offers a rapid and facile means for decorating CNTs with metal nanoparticles. Usually, the entire deposition process lasts from a couple of seconds to several minutes. Nonetheless, it is noteworthy that the electrodeposition is not necessarily site-selective as the tips/ends and sidewalls may be plated equally well under the conditions employed. Moreover, most of the literature associated with the synthesis of CNT–nanoparticle heterostructures fabricated *via* electrodeposition tend to be limited to the use of noble metals, such as Pd,[145–147] Pt,[143,147,148] Au,[147] and Ag.[149] Nonetheless, to a lesser extent, work on metal oxides[150] has proceeded as well. For example, the electrodeposition of TiO_2 from aqueous $TiCl_3$ solution results in solid electrodes where the SWNT bundles are covered with anatase TiO_2 crystals. In addition, recently, low field–high current and high field–low current electrophoretic deposition techniques were integrated successfully in an alternating sequence to fabricate multilayered porous carbon nanotube–densely packed Fe_3O_4 nanocrystal composite films.[151]

A typical experiment[143] for the deposition of Pt nanoparticles onto SWNTs involves an initial gentle oxidation followed by electrochemical treatment without damage to the CNT surface. Complexes of Pt(IV) can then be formed with carboxylate groups on the SWNT surface under conditions of cyclic voltammetry, followed by transformation into well-dispersed Pt nanoparticles, possessing a diameter range of 4–6 nm.[143] The electrochemical properties of Pt–SWNT composites for methanol oxidation were subsequently examined. Two peaks of methanol oxidation, located at 0.89 and 0.45 V, were observed in the case of Pt/SWNT paste electrodes, but not when SWNTs were used alone. Later on, the same group generated Pd/SWNT nanocomposites electrochemically, based on the same principle, ascribing the improved performance in that system to the small particulate size and high dispersion of the Pd nanoparticles, providing for a multitude of surface active sites.[146] A coating of poly(vinylidene fluoride) cast on a forest of aligned MWNTs electrodeposited with Pt nanoparticles also yielded an efficient, robust, and high surface area electrocatalyst.[152]

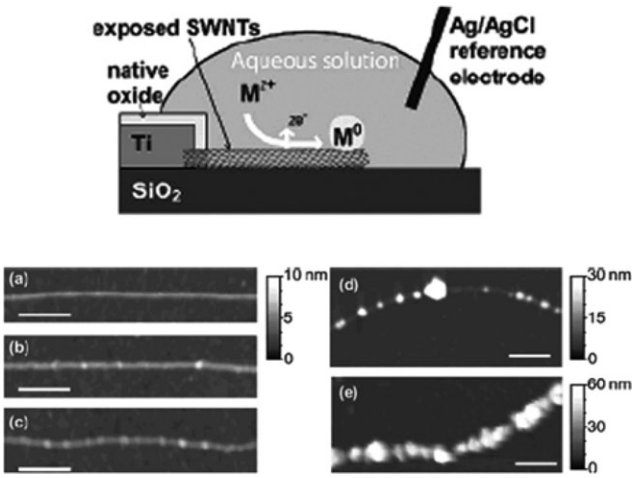

Fig. 9 (Top) Schematic illustration of the SWNT electrode. (Bottom) AFM images obtained in air pre (a) and post Au deposition at varying nucleation potentials: (b) 0.2, (c) −0.2, (d) −0.4 and (e) −0.8 V *vs.* Ag/AgCl at separate nominally identical SWNT electrode devices. Deposition time was 20 s. Scale bar = 300 nm. Reprinted with permission from B. M. Quinn, C. Dekker and S. G. Lemay, *J. Am. Chem. Soc.*, 2005, **127**, 6146. Copyright 2005, American Chemical Society.

Quinn *et al.*[147] designed a device (Fig. 9) containing a SWNT electrode, wherein the SWNTs served a dual purpose: initially as the electrodeposition template and subsequently as a wire to electrically connect the deposited Au, Pt and Pd nanoparticles. It was found that the density and the size of the metal clusters could be tuned to a large extent by careful choice of the applied potential, deposition time, and metal salt concentration. For instance, small clusters with heights of ~6 nm could be generated at low surface sidewall coverage using a small positive nucleation potential, E of 0.2 V, whereas clusters of larger average heights measuring 60–90 nm and uniformly covering the nanotube sidewall could be formed with a negative nucleation potential, $E = -0.8$ V.

To investigate the nucleation and growth mechanisms of aqueous solutions of noble metals on SWNTs under electrochemical control, Day *et al.*[149] constructed two types of devices, in which SWNTs served as the electrode. Using direct electrodeposition, it was possible to control the density and size of the metal nanoparticles using the applied potential and time. In studies using an uninsulated gold contact exposed to solution, essentially contiguous nanowires were observed to materialize along SWNTs near the contacts with isolated discrete nanoparticles found to form further away. Au growth was found to be rapid and progressive with an increasing nanoparticle density over time. Conversely, Pt deposition was characterized by lower nucleation densities and slower growth rates with a tendency for a higher density of larger particles to be produced over longer periods of reaction time.

2.3.4 Complementary formation protocols. In terms of other developed protocols, sonochemistry in acid has been utilized to generate SWNTs[153] with a uniformly high dispersion of Pt nanoparticles, possessing sizes of less than 5 nm and loading values of up to 30 wt% with little aggregation. It was claimed that the sonochemical process not only prevented a

Published on 13 February 2009. Downloaded by Pennsylvania State University on 12/09/2016 18:00:11.

degree of nanotube aggregation but also led to the presence of uniform surface functional sites on all of the nanotubes, thereby allowing for the subsequent deposition of well-dispersed nanoparticles. Au and Ag clusters have been deposited onto nanotube surfaces by similar means.[154] Average Pt nanoparticle sizes were noted to be 2.78 ± 0.86, 3.57 ± 0.78 and 4.46 ± 1.33 nm for the 10, 20, and 30 wt% catalysts, respectively. Au has been successfully deposited on MWNTs at levels of up to 50 wt% by sonication in the presence of a stabilizer, *i.e.* tetrakis(hydroxymethyl)phosphonium chloride; the resulting composites were active catalysts in transformations of methyoxirane.[155] Acid-treated MWNTs have also been decorated with <5 nm Sn nanoparticles[156] by exposure to a solution of $SnCl_2$ in EG under N_2 atmosphere.

The combination of microwave radiation (Fig. 10) with polyol reduction of the Au salt, without the use of an aggressive oxidation treatment, in a single processing step[157] has been used to derivatize CNTs with Au nanoparticles. As-prepared nanoparticles coated the CNT surface uniformly with an average size of 6 ± 0.7 nm. It has even been shown[158] that chemical modification of CNTs is not necessarily a pre-condition for the decoration of nanoparticles onto CNT surfaces. For example, the heterogeneous nucleation and growth of dense and uniformly dispersed Pt nanoparticles on unmodified CNTs with a loading of 50 wt% was realized, owing to the salt effect of SDS. By changing either the concentration of metal ions, the reaction temperature, the reducing agent, or the means of adding reagents, the size of Pt nanoparticles could be controlled precisely and deliberately to a size range of 2.3 to 9.6 nm.

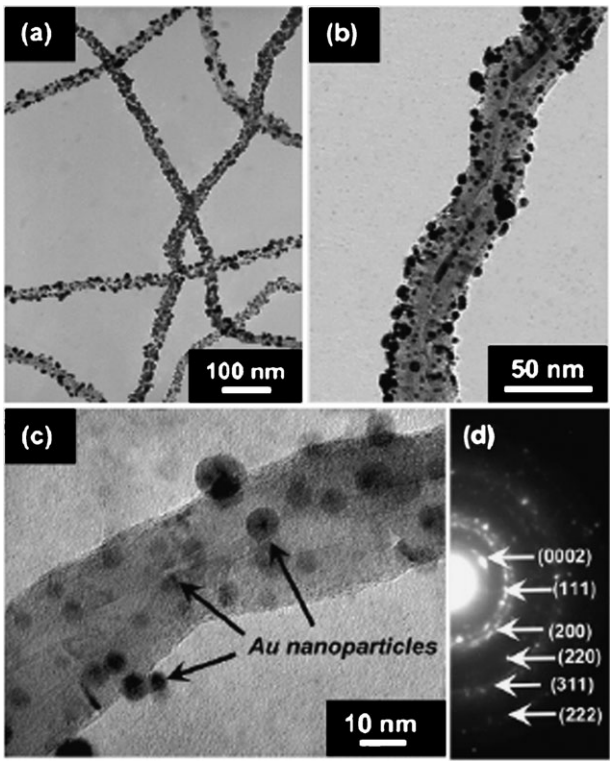

Fig. 10 (a, b) Low- and (c) high-magnification bright-field TEM micrographs illustrating the decoration of multiwalled CNTs with 3–10 nm diameter Au nanoparticles. Note that the hollow of the tubes remains intact, indicating that the overall structure of the CNTs is preserved. (d) Selected area electron diffraction pattern showing diffraction spots corresponding to the (0002) basal planes of the CNTs and rings corresponding to polycrystalline fcc Au nanoparticles. Reprinted with permission from M. S. Raghuveer, S. Agrawal, N. Bishop and G. Ramanath, *Chem. Mater.*, 2006, **18**, 1390. Copyright 2006, American Chemical Society.

Aligned MWNTs have been coated with TiO_2 nanoparticles using atmospheric pressure chemical vapor deposition (CVD).[159] Gold nanoparticles have been embedded into the walls of CNTs using a template-assisted CVD process.[160] Even individual 8 nm diameter cobalt and tungsten nanoparticles have been distributed onto nanotube surfaces using this technique with the growth properties found to depend on precursor decomposition temperature, nanotube length, thermal conductivity, convective and radiative losses, as well as nanotube heating characteristics.[161] Using a gas-phase route, *i.e.* an aerosol source of nanoparticles,[162] but in the presence of an electrostatic force field, SnO_2 and Ag nanocrystals have been attached to MWNTs with demonstrated control over size, packing density, and size distribution.[163] Moreover, focused-ion-beam irradiation and a subsequent mild chemical treatment have been used to site selectively functionalize MWNTs with Au nanoparticles.[164]

2.3.5 Summary of protocols leading to approaches for the direct formation of NPs onto CNTs. These strategies are highly effective towards creating nanotube–nanocrystal composites and are generalizable to the use of all types of semiconducting and metallic nanoparticles. Moreover, in many cases, the inherent properties of the nanocrystals and nanotubes are preserved to a high degree, thereby allowing for their efficacious incorporation into practical devices such as catalysts. Yet, it is also clear that some of these protocols can be potentially inconvenient and harsh, as they may involve either toxic, unstable, or highly reactive precursors as well as expensive instrumentation. Moreover, the mechanism for synthesizing these heterostructures is not always well known and hence, it can be difficult to adequately predict the resulting nanotube–nanoparticle morphology and composition. In this regard, it may be even more challenging to conceive of controlling the spatial location and density of nanoparticle growth on such nanotube templates using these methods.

3 Selected applications of nanotube–nanocrystal hybrids

Based on the nature of nanocrystals produced, there are three types of nanotube–nanocrystal hybrid systems, including CNT–metal nanoparticles, CNT–quantum dots, and CNT–metal oxide nanoparticles. In the best possible case, therefore, conjugation of these nanoparticles onto CNT templates should not only preserve the favorable size-dependent properties of zero-dimensional nanomaterials but also greatly enhance the intrinsic optoelectronic and mechanical properties of one-dimensional nanotube motifs. The potential here is that one can create a tailorable, nanoscale heterostructure with novel and potentially unforeseen properties. We have often spoken thus far of interesting

 This journal is © The Royal Society of Chemistry 2009

Published on 13 February 2009. Downloaded by Pennsylvania State University on 12/09/2016 18:00:11.

performance enhancement (especially, catalytic) associated with the products of many of the synthetic protocols we have already described. As a typical example,[165] ZnO-coated MWNT nanocomposites exhibit enhanced photocatalytic activity with respect to the photocatalytic degradation of Methylene Blue. In the following sections, we highlight key advances denoting how classes of nanotube–nanocrystal heterostructures can conceivably be incorporated into practical device applications.

3.1 CNT–metal nanoparticle heterostructures

One of the first reported applications[166] for carbon nanotubes involved their use as supports for 3–7 nm Ru nanoparticles in the heterogeneous catalysis involving hydrogenation of cinnamaldehyde. Although the mechanism still remains unclear, the reaction involved a noticeably higher selectivity (>92%) for cinnamyl alcohol generation as compared with the use of Ru supported either on Al_2O_3 (20–30%) or on active carbon (30–40%). Since then, the vast majority of applied studies involving metal-nanoparticle deposition on CNTs have been associated with nanotubes coupled to Pt, Pd, Ru, Ag and Au, especially because the intrinsic nature of these transition metals renders them useful in areas as diverse as catalysis, hydrogen storage, fuel cell technology, and sensing.[144] As an example, a membrane electrode assembly incorporating Pt–SWNTs for use in hydrogen fuel cells was shown to exhibit a ~20% improvement in maximum power density.[167] In a different set of studies, Pt-coated, polymer-wrapped SWNTs not only were found to be reasonably stable[168] but also possessed a two-fold higher catalytic activity for oxygen reduction[141] as compared with conventional materials. In this critical review, though, we will focus primarily on the use of these metal nanoparticle–nanotube heterostructures for effective chemical sensing.

3.1.1 Chemical sensors. Chemical sensing typically relies on strong interactions between a sensor material and its target analyte(s). Adsorption interactions generally result in a degree of charge transfer between gaseous molecules and the interacting nanotubes, causing a dramatic change in conductivity that can be subsequently detected.[169] Hence, electron donating and withdrawing molecules will either transfer electrons to or attract electrons from SWNTs, thereby providing for either additional charge carriers or holes that are reflected in their measured conductance. However, not all molecules (such as methane with its poor electron accepting/donating properties), that are nevertheless of high interest to environmental monitoring, industrial chemical processes, as well as agricultural and biomedical applications, can be probed in such a manner. In this regard, chemical decoration of SWNTs with metal nanoparticles has often been an important route forward towards resolving this issue and enhancing detection. In fact, theory predicts that nanotube–Al cluster systems, for instance, facilitate the adsorption of both ammonia[170] and CO,[171] and that Ru-decorated SWNTs enhance the detection of carbon monoxide.[172]

Experimentally, Pd-modified (using e-beam evaporation) SWNTs have been found to exhibit significant but highly reversible electrical conductance modulation upon exposure to small concentrations of H_2 in air at room temperature. Sensitivities (defined as the ratio between the resistance before and after gas exposure) to 400 ppm H_2 were found to be ~2 with response times (defined as the time duration over which half of the measured resistance change occurred) of 5–10 s and a full recovery time in air of ~400 s.[173] Recently, it was reported[174] that a SWNT network, decorated with Pd nanoparticles, whose synthesis was optimized by varying electrodeposition charge and potential conditions, exhibited excellent sensing performance of hydrogen with a lower detection limit of 100 ppm and a linear response up to 1000 ppm. The response time ranged from a few to tens of minutes depending upon the hydrogen concentration, but the observed recovery time of the device was found to improve with increased humidity. High performance, mechanically flexible hydrogen sensors have been constructed from SWNTs electrodeposited with Pd nanoparticles.[175] These were typically associated with a sensitivity of ~75% for 500 ppm hydrogen in air and a response time of ~3 s for 1% hydrogen at room temperature.

SWNTs loaded with Pd nanoparticles have also been utilized for the detection of CH_4 ranging from 6 to 100 ppm in air at room temperature. These sensors exhibited reduced size, lower power consumption (factor of 100), and higher sensitivity (factor of 10), as compared with conventional catalytic beads and metal oxide sensors for methane detection.[176] The sensing mechanism was proposed as arising from electron transfer from SWNTs to Pd, resulting in the formation of a long-range, weakly bound complex of $Pd^{\delta+}(CH_4)^{\delta-}$ at room temperature. MWNTs coated with Pd demonstrated a response magnitude of ~4.5% towards 2% methane at room temperature.[177] Metastable bamboo MWNTs decorated with <1 nm Pd nanoparticles have been used to sense hydrazine in the pH range, where Pd would normally have been oxidized on the surface of conventional electrodes.[178]

Sensor arrays have been constructed by site-selectively electroplating Pd, Pt, Rh and Au metals on isolated SWNT networks on a single chip. In total,[179] 18 catalytic metals were used for the detection of H_2, CH_4, CO and H_2S gases. In addition, SWNT films modified with Au nanoparticles have been used for the ultrahigh sensitive detection of NO_2 under ambient conditions.[180] The detection limit of NO_2 improved 9.6-fold to 4.6 ppb as compared with that obtained using pure SWNT sensors alone. Optically transparent and electrically conductive nanocomposite thin films composed of MWNTs, Au nanoparticles, and myoglobin molecules can vary their resistance, impedance, or optical transmittance, respectively, at room temperature in response to changes in ambient humidity and water absorption to as much as four times greater than typically exhibited by conventional structures including myoglobin-functionalized MWNT thin films.[181] By analogy, nanohybrid films[182] composed of MWNTs, gold nanoparticles and hemoglobin have been used to construct a stable, reproducible third-generation H_2O_2 biosensor with a linear range from 2.1×10^{-7} to 3.0×10^{-3} M and a detection limit down to 8.0×10^{-8} M.

3.2 Applications of CNT–quantum dot heterostructures

3.2.1 Solar applications. In quantum dots (0-d systems), as discussed, the absorption spectrum is tunable by changing the

Published on 13 February 2009. Downloaded by Pennsylvania State University on 12/09/2016 18:00:11.

size of the quantum dot.[23,24] An ensemble of quantum dots of different sizes can therefore in principle be designed to match the ensemble absorption spectrum to the solar spectrum. Moreover, though controversial,[183] an intriguing recent discovery is that of multiple exciton generation in quantum dots which effectively converts a photon into more than one electron–hole pair allowing for more efficient use of solar energy and a potential for quantum efficiencies greater than 100%.[184–186] By contrast, CNTs can transport charge ballistically over relatively large distances at room temperature.[187–189] That is, in these 1-D systems, the charge collection efficiency might be enhanced due to enhanced charge transport. In general though, one individual nanoscale component will have some but not all of the desired properties needed for enhanced overall solar energy utilization. For example, while quantum dots can lead to higher quantum efficiency, an isolated dot must have the excitations removed and charges separated to be useful. Hence, there has been a strong interest in developing hybrids of CNTs and semiconducting quantum dots in recent years.

We ourselves have shown that the properties of the assembled zero-dimensional–one-dimensional composite system are different from the simple sum of its parts. A significant observation from our lab is the quenching of luminescence emission from a quantum dot when in close proximity to the nanotube.[52] This has suggested the feasibility of rapid energy transfer to the nanotube. This phenomenon seems to depend only on the relative separation of the nanotube and quantum dot as it has been observed with previously discussed chemical linkers,[52,58] direct sidewall growth,[108] and polymer spacers.[79] However, it is interesting to note that in cases where an inorganic dielectric layer was used to either cap the nanotube or the quantum dot, the fluorescence is recovered.[190] In general, there seems to be only a weak perturbation of the electronic states of either system as absorption measurements have shown little or no shifts in the electronic transition energies.[58] As it appears that the electronic coupling between the 0D and 1D systems is weak, then the likely mechanisms for fluorescence quenching involves tunneling of the carriers out of the nanocrystal or resonance energy transfer between the two systems. Both processes have been shown to be important in natural photosynthetic systems and have distinctive time, energy and length scales.[191]

As we initially discussed in section 2.1.1, the bulk of studies have therefore focused on quantum dots attached to SWNT templates. These semiconducting nanostructures have included CdS, CdSe, CdTe and PbSe. In this section, we will highlight additional advances in the area. It should be mentioned though that strong electronic coupling was also observed in dispersible nanotube-gold nanoparticle composites.[82] Moreover, upon excitation with UV light, ZnO particles[192] will undergo charge separation and inject electrons into carboxylic acid-functionalized nanotubes with a rate constant of 1×10^8 s^{-1}.

For example, Willner and collaborators[193] fabricated CdS/CNT hybrid composites on a Au electrode. The CdS NPs, stabilized by a mixed monolayer of cysteamine and 2-thioethanol in a 3 : 1 molar ratio, were covalently coupled to the carboxylic acid groups at the ends of the oxidized CNTs, processed according to a HNO_3–H_2SO_4 acidic treatment. From the intensity of the light absorbed by the sample, the quantum efficiency for photon-to-electron conversion was measured to be 25%, as compared with the 1.5% value noted for nanotubes alone. A high quantum efficiency of the CdS nanocrystals (70%) was achieved upon acid digestion times of up to 10 h. These results suggested that the lengths of CNTs play an important role in the formation of photocurrent with longer nanotubes associated with a higher density of defects and therefore, lower quantum yields.

In another study on a similar hybrid system,[109] Kamat and co-workers used an electrophoretic deposition approach to cast films of SWNTs onto optically transparent electrodes and chemically precipitated CdS onto the nanotube surface. As with the prior work,[193] the observed photocurrent was dominated by the initial excitation of the CdS. Specifically, the interaction between CdS and the SWNT was probed using both emission and transient absorption spectroscopy. The CdS colloids exhibited emission in the red with a maximum of around 670 nm. This red-light emission was thought to arise from the sulfur vacancy of CdS colloids and could be used to monitor the charge-separation and charge-recombination processes following bandgap excitation. Nonetheless, the emission of CdS could be totally quenched when bound to the SWNTs, suggesting a strong excited-state interaction with the nanotube with the deactivation process thought to occur *via* electron transfer to the nanotube. From bleaching data, electron transfer rate constants were noted to be 4×10^8 s^{-1} with low photon-to-charge carrier generation efficiencies.[109] Thus, the authors proposed that photocurrent production was likely a net effect of the initial, fast charge transfer from the CdS to the SWNTs, followed by charge transport to the optically transparent electrode, and later, a slower regeneration of the CdS through the redox couple. Relatively low IPCE values ($<1\%$) were suggestive of inherent problems associated with charge collection and charge transport in those SWNT–CdS films.

Interesting charge transfer behavior has also been noted in additional systems studied by Kamat and co-workers (Fig. 11). For instance, in the analogous TiO_2–SWNT system, in which the nanotubes directed the flow of photogenerated charge carriers, the photoconversion efficiency was increased by a factor of two with a shift of $\sim$100 mV in the apparent Fermi level of the TiO_2–SWNT system as compared with an unsupported TiO_2 scaffold.[194] When in contact with photo-irradiated TiO_2 nanoparticles, SWNTs can accept and store electrons. Fermi level equilibration with these particles indicated storage of up to 1 electron per 32 carbon atoms and the stored electrons could be readily discharged upon addition of electron acceptors such as thiazine and oxazine dyes.[195] It should be noted though that in a separate experiment, the same group did not find that the presence of SWNTs, when used as a support architecture, interfered with the charge injection process of an excited Ru(II) tris-bipyridyl complex into nanoscale TiO_2 particles.[196]

As previously described, Prato *et al*. systematically devised and tested CNT/pyrene$^+$/CdTe conjugates as donor-acceptor nanohybrids in dilute condensed media and as integrative

 This journal is © The Royal Society of Chemistry 2009

Published on 13 February 2009. Downloaded by Pennsylvania State University on 12/09/2016 18:00:11.

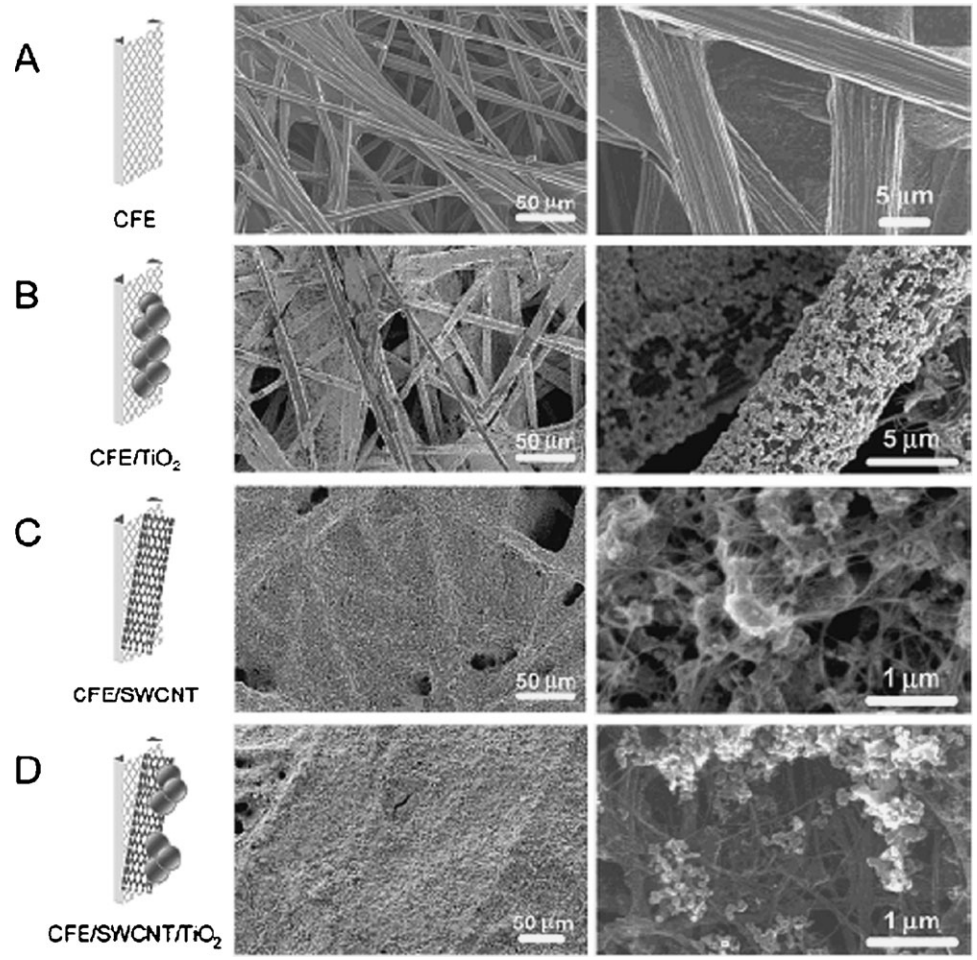

Fig. 11 SEM of a carbon fiber electrode (CFE) at different stages of modification: (A) before surface modification; (B) after modification with TiO_2 particles; (C) after electrophoretic deposition of SWNT; (D) after deposition of TiO_2 particles onto SWNT film. Reprinted with permission from A. Kongkanand, R. M. Dominguez and P. V. Kamat, *Nano Lett.*, 2007, **7**, 676. Copyright 2007, American Chemical Society.

components at electrode surfaces.[97] Strong electronic interactions in the ground and excited states were thought to be responsible for the favorable charge-transfer characteristics observed. In response to visible light irradiation, SWNT/pyrene$^+$/red CdTe and SWNT/pyrene$^+$/green CdTe exhibited 11.5- and 7.2-fold amplification, respectively, of the photocurrent, relative to that observed in the absence of CdTe. In essence, photoexcitation of CdTe led to a subsequent electron injection into electron accepting SWNTs. Notably, the nanotubes acted as charge delivery channels, rapidly transporting the charge carriers from the photogeneration point to the ITO electrode. Interestingly, it was noted that the sequence of deposition, creating either CNT/pyrene$^+$/red CdTe or red CdTe/CNT/pyrene$^+$ structures, had a profound effect on the resulting photocurrent mechanism. In a complementary experiment, the Stoddart and Grüner groups[197] demonstrated effective charge transfer from pyrene/CdSe nanoparticles using both fluorescence quenching experiments and transistor measurements with the magnitude of the charge transfer observed noted to be dependent on the light intensity and wavelength. A maximum of 2.2 electrons per pyrene/CdSe nanoparticle was recorded.

CdSe and SWNTs have also been incorporated into a poly(3-octylthiophene)–(P3OT) composite in order to facilitate exciton dissociation and carrier transport in a proper device architecture.[198] In this complex three-dimensional network structure, photoinduced excitons in the polymer are expected to be dissociated by the nearest high electron affinity material, namely either a quantum dot or a SWNT. Ultimately, the holes will be transported by the polymer to the positive electrode and the dominant electron path should be through the percolating SWNTs to the negative electrode. The point is that the degree to which the quantum dots can produce excitons as well as the degree to which SWNTs and the polymer can absorb light and thereby create bound electron–hole pairs ultimately determine the nature and tunability of the types of junctions that can be created. All of these parameters though are fundamentally a function of the precise morphology (*e.g.* diameter, type, size) of each of the individual building blocks of this solar cell architecture.

3.2.2 Drug delivery. A number of approaches to the functionalization of CNTs with biomolecules on their external surface have been reported for potential applications in drug

Published on 13 February 2009. Downloaded by Pennsylvania State University on 12/09/2016 18:00:11.

delivery. As examples of their versatility, SWNTs non-covalently bound to proteins or genes mediated by phospholipids were internalized into cells through endocytosis.[199–204] SWNTs can also be covalently functionalized with small molecules linked to the carboxylic acid sites localized at their ends, defect sites, or sidewalls.[205] Thus, amino acids,[206] oligopeptides,[207–210] genes,[211–213] and antibiotics[214] have been effectively transported into different types of living cells *via* appropriately functionalized SWNTs.[215] Nonetheless, in order to track such conjugates in a living system, a fluorescent dye is commonly used as a tagging label. However, the disadvantage of this approach is the low quantum yield and short lifetime of dye molecules upon interaction with these species. For this reason, quantum dots[216] have often been used to replace organic dyes and to visualize[217] various molecules in biosystems both under *in vitro* and *in vivo* conditions. Not surprisingly, quantum dots[68] and iron oxide nanoparticles[218] have recently been attached to carbon nanotubes to form bioimaging agents that can then be readily visualized using fluorescence microscopy and magnetic resonance/near IR fluorescence techniques, respectively.

As we have described earlier, Bottini *et al.* demonstrated that streptavidin conjugated quantum dots could be adsorbed on the surface of the SWNTs, forming a supramolecular nanostructure fully dispersible in physiological buffer solution.[55] This SWNT/streptavidin-conjugated quantum dot could be used not only as a multivalent intracellular fluorescent nanoprobe but also as a targeted delivery vehicle with enhanced loading capacity as compared with small molecules. This conjugate nanoassembly was delivered internally into Jurkat T leukemia cells through a biotinylated anti-CD3 antibody (present in the incubation solution), CD3 receptor (associated with the cell membrane) mediated endocytosis. Once internalized into the cells, the nanoassembly was eventually transported to lysosomes. What is significant is that this luminescent nanoassembly was clearly visible using both optical and confocal fluorescent microscopies.

Alternatively, the quantum dots can be attached to the biomolecules themselves, followed by assembly onto the SWNT surface. For instance, Jia *et. al.* have recently shown that antisense oligodeoxynucleotide-tagged CdTe (ASODNs–CdTe) nanocrystals can electrostatically interact with cationic polyelectrolyte functionalized MWNTs (*e.g.* MWNTs–PEI) to form a carbon nanotube delivery system capable of delivering therapeutic genes into the nuclei of cells.[219] A combination of confocal microscopy imaging and flow cytometry analysis enabled the qualitative and quantitative assay of MWNTs–ASODNs–CdTe conjugate delivery into HeLa cells. Specifically, confocal imaging and accompanying intense fluorescence showed that CdTe-labeled ASODNs–MWNTs–PEI localized mainly in the cell nucleus, whereas flow cytometry analysis indicated that MWNTs–PEI could result in a delivery of ASODNs (which were subsequently found to show effective anticancer activity) by CdTe quantum dots with an efficiency approaching 95%. All of these data (Fig. 12) were in support not only of an endocytosis mechanism for cellular uptake of these conjugates but also for the promise of using a highly visualizable, fluorescently tagged CNT platform for biological drug delivery and gene therapy applications.

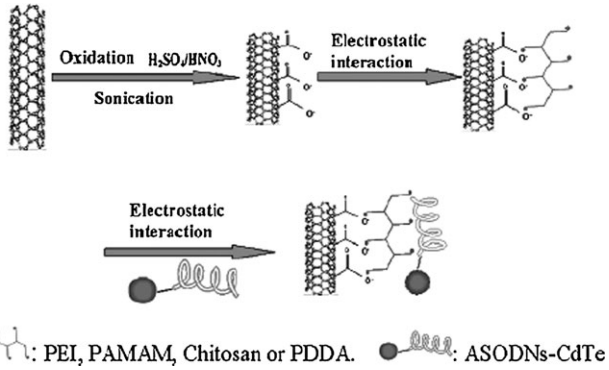

Fig. 12 Approach and mechanism for preparing MWNT–PEI–ASODNs–CdTe. Reprinted with permission from N. Q. Jia, Q. Lian, H. B. Shen, C. Wang, X. Y. Li and Z. N. Yang, *Nano Lett.*, 2007, **7**, 2976. Copyright 2007, American Chemical Society.

3.3 Applications of CNT–metal oxide heterostructures

There are a number of diverse applications that have incorporated metal oxide nanoparticles onto nanotube templates; we have already described some of these. Energy-related applicability is a consistent theme. For example, whereas unfunctionalized MWNT supercapacitors will yield a specific capacitance of $\sim$67 F g^{-1}, the corresponding RuO_2/MWNT, TiO_2/MWNT and SnO_2/MWNT nanocrystalline composites developed as supercapacitor electrodes have resulted in specific capacitances of $\sim$138, 160 and 93 F g^{-1}, respectively.[220] The enhancement observed as compared with pure MWNTs has been attributed to the progressive redox reactions occurring at the surface and bulk of transition metal oxides through Faradaic charge-transfer due to modification of the nanotube surface by the oxide nanomaterials. Furthermore, TiO_2/CNT systems in particular have been sought as a model case for Li-battery applications.[221] Electrochemical testing indicated that the reversible capacity of this cathode material could be maintained at about 225 mA h g^{-1}, about 17% higher than that reported for hydrogen titanate nanowires (191.8 mA h g^{-1}), about 32% higher than that for nanosized rutile TiO_2 ($\sim$170 mA h g^{-1}), and as much as 50% greater than that for anatase TiO_2 ($\sim$150 mA h g^{-1}) alone.

4 Summary and outlook

In summary, the area of carbon nanotube–nanocrystal heterostructures has evolved from merely being a subject of esoteric scientific curiosity to one that has gained broad applicability, acceptance, and serious interest in recent years. In this review, we have extensively described a number of diverse approaches and strategies for the generation of carbon nanotube–nanocrystal heterostructures, including not only covalent and noncovalent approaches but also *in situ* synthesis techniques, all of which have been aimed at reproducibly and reliably immobilizing nanocrystals onto the surfaces of CNTs. Indeed, the rational fabrication of carbon nanotube–nanoparticle heterostructures in terms of size, shape, morphology, crystallinity and chemical composition remains an active area of study. Fundamentally, the importance of generating a true

 This journal is © The Royal Society of Chemistry 2009

Published on 13 February 2009. Downloaded by Pennsylvania State University on 12/09/2016 18:00:11.

nanoscale heterostructure with properties that transcend the isolated properties of its constituent components is one major motivation for continuing this line of scientific pursuit. That is, the properties of carbon nanotube–nanocrystal heterostructures are not merely the simple sum of their parts; the potential enhancement in favorable properties in these discrete systems could impact a wide range of areas including catalysis, sensing, optoelectronic devices, drug delivery, and biolabeling. We also believe that this will be a key architecture in the ongoing struggle to develop improved energy storage devices as well as alternative power sources (such as efficient solar cells).

In this review, the advantages and/or disadvantages of each synthesis approach have been discussed, shining light on plausibly appropriate ways for fabricating desirable heterostructures for specific applications. Each of these experimental methods in principle has an underlying goal, namely that of improving the physical, chemical, and biological properties of the resulting heterostructure. Nonetheless, further effort is still needed in a number of parallel areas.

First, it is difficult to control the rate, density, and spatial localization of functionalization of nanocrystals onto nanotube templates. Second, the nature (and adequate detection) of defects in these systems is not well understood. Third, the exact growth mechanisms involved with most of the synthetic methods used for creating heterostructures are often a matter of speculation. For instance, it is empirically known that factors such as temperature, heating rates, ionic strength, solvent viscosity, as well as the presence of organic ligands play an important role in determining the morphology of the final products, depending on the protocol. However, the exact mechanism of how each individual variable precisely correlates with overall nanoparticle growth on the nanotube template is rarely known. Fourth, the issue of large-scale production of such nanomaterial heterostructures remains very much unresolved, though it will be key to promoting their widespread applicability. Fifth and likely most importantly, health, toxicity, and environmental issues associated with the various synthetic protocols of the as-obtained nanomaterials will need to be addressed in a timely fashion, if the general public is to feel genuinely comfortable with and accepting of these practical heterostructure-based nanoscale devices in everyday life.

Acknowledgements

We acknowledge the US Department of Energy (DE-AC02-98CH10886) for facility and personnel support. We also thank the National Science Foundation (CAREER Award DMR-0348239), and the Alfred P. Sloan Foundation for support and experimental supplies.

References

1 S. Iijima, *Nature*, 1991, **354**, 56.
2 M. S. Dresselhaus, G. Dresselhaus and P. Avouris, *Carbon Nanotubes: Synthesis, Structure, Properties, and Applications*, Springer-Verlag, Berlin, 2001.
3 R. Saito, G. Dresselhaus and M. S. Dresselhaus, *Appl. Phys. Lett*., 1992, **60**, 2204.
4 J. W. Mintmire, B. I. Dunlap and C. T. White, *Phys. Rev. Lett*., 1992, **68**, 631.
5 T. W. Odom, J.-L. Huang, P. Kim and C. M. Lieber, *Nature*, 1998, **391**, 62.
6 O. Lourie and H. D. Wagner, *J. Mater. Res*., 1998, **13**, 2418.
7 A. Krishnan, E. Dujardin, T. W. Ebbesen, P. N. Yianilos and M. M. J. Treacy, *Phys. Rev. B*, 1998, **58**, 14013.
8 S. J. Tans, M. H. Devoret, H. J. Dai, A. Thess, R. E. Smalley, L. J. Geerligs and C. Dekker, *Nature*, 1997, **386**, 474.
9 J. Chen, V. Perebeinos, M. Freitag, J. Tsang, Q. Fu, J. Liu and P. Avouris, *Science*, 2005, **310**, 1171.
10 C. Wang, M. Waje, X. Wang, J. M. Tang, R. C. Haddon and Y. S. Yan, *Nano Lett*., 2004, **4**, 345.
11 A. Bachtold, P. Hadley, T. Nakanishi and C. Dekker, *Science*, 2001, **294**, 1317.
12 V. Lordi, N. Yao and J. Wei, *Chem. Mater*., 2001, **13**, 733.
13 J. M. Planeix, N. Coustel, B. Coq, V. Brotons, P. S. Kumbhar, R. Dutartre, P. Geneste, P. Bernier and P. M. Ajayan, *J. Am. Chem. Soc*., 1994, **116**, 7935.
14 R. H. Baughman, C. X. Cui, A. A. Zakhidov, Z. Iqbal, J. N. Barisci, G. M. Spinks, G. G. Wallace, A. Mazzoldi, D. De Rossi, A. G. Rinzler, O. Jaschinski, S. Roth and M. Kertesz, *Science*, 1999, **284**, 1340.
15 R. H. Baughman, A. A. Zakhidov and W. A. de Heer, *Science*, 2002, **297**, 787.
16 S. Fan, M. G. Chapline, N. R. Franklin, T. W. Tombler, A. M. Cassell and H. Dai, *Science*, 1999, **283**, 512.
17 Q. Zhao, Z. H. Gan and Q. K. Zhuang, *Electroanalysis*, 2002, **14**, 1609.
18 J. Kong, N. R. Franklin, C. W. Zhou, M. G. Chapline, S. Peng, K. J. Cho and H. Dai, *Science*, 2000, **287**, 622.
19 C.-M. Yang, H. Kanoh, K. Kaneko, M. Yudasaka and S. Iijima, *J. Phys. Chem. B*, 2002, **106**, 8994.
20 S. S. Wong, E. Joselevich, A. T. Woolley, C. L. Cheung and C. M. Lieber, *Nature*, 1998, **394**, 52.
21 R. Saito, G. Dresselhaus and N. Dresselhaus, *Physical Properties of Carbon Nanotubes*, Imperial College, London, 1998.
22 L. Brus, *Appl. Phys. A*, 1991, **53**, 465.
23 A. P. Alivisatos, *J. Phys. Chem*., 1996, **100**, 13226.
24 C. B. Murray, D. J. Norris and M. G. Bawendi, *J. Am. Chem. Soc*., 1993, **115**, 8706.
25 M. Bruchez, M. Moronne, P. Gin, S. Weiss and A. P. Alivisatos, *Science*, 1998, **281**, 2013.
26 D. H. Marsh, G. A. Rance, R. J. Whitby, F. Giustiniano and A. N. Khlobystov, *J. Mater. Chem*., 2008, **18**, 2249.
27 P. L. McEuen, *Nature*, 1998, **393**, 15.
28 S. Saito, *Science*, 1997, **278**, 77.
29 E. Unger, G. S. Duesberg, M. Liebau, A. P. Graham, R. Seidel, F. Kreupl and W. Hoenlein, *Appl. Phys. A*, 2003, **77**, 735.
30 S. Ravindran and C. S. Ozkan, *Nanotechnology*, 2005, **16**, 1130.
31 H. Lee, S. W. Yoon, E. J. Kim and J. Park, *Nano Lett*., 2007, **7**, 778.
32 L. Kavan, P. Rapta and L. Dunsch, *Chem. Phys. Lett*., 2000, **328**, 363.
33 J. L. Bahr and J. M. Tour, *Chem. Mater*., 2001, **13**, 3823.
34 J. L. Bahr, J. Yang, D. V. Kosynkin, M. J. Bronikowski, R. E. Smalley and J. M. Tour, *J. Am. Chem. Soc*., 2001, **123**, 6536.
35 S. Banerjee and S. S. Wong, *Adv. Mater*., 2004, **16**, 34.
36 M. S. Dresselhaus, G. Dresselhaus, A. Jorio, A. G. Souza Filho, M. A. Pimenta and R. Saito, *Acc. Chem. Res*., 2002, **35**, 1070.
37 Z. Yu and L. E. Brus, *J. Phys. Chem. B*, 2001, **105**, 1123.
38 M. S. Strano, C. A. Dyke, M. L. Usrey, P. W. Barone, M. J. Allen, H. W. Shan, C. Kittrell, R. H. Hauge, J. M. Tour and R. E. Smalley, *Science*, 2003, **301**, 1519.
39 J. L. Bahr and J. M. Tour, *J. Mater. Chem*., 2002, **12**, 1952.
40 S. Banerjee and S. S. Wong, *J. Phys. Chem. B*, 2002, **106**, 12144.
41 S. H. Hwang, C. N. Moorefield, P. S. Wang, K. U. Jeong, S. Z. D. Cheng, K. K. Kotta and G. R. Newkome, *J. Am. Chem. Soc*., 2006, **128**, 7505.
42 V. Biju, T. Itoh, Y. Baba and M. Ishikawa, *J. Phys. Chem. B*, 2006, **110**, 26068.
43 D. L. Shi, Y. Guo, Z. Y. Dong, J. Lian, W. Wang, G. K. Liu, L. M. Wang and R. C. Ewing, *Adv. Mater*., 2007, **19**, 4033.
44 M. Scolari, A. Mews, N. Fu, A. Myalitsin, T. Assmus, K. Balasubramanian, M. Burghard and K. Kern, *J. Phys. Chem. C*, 2008, **112**, 391.

Published on 13 February 2009. Downloaded by Pennsylvania State University on 12/09/2016 18:00:11.

45 D. Gal, Y. Mastai, G. Hodes and L. Kronik, *J. Appl. Phys.*, 1999, **86**, 5573.
46 I. Mora-Sero, J. Bisquert, T. Dittrich, A. Belaidi, A. S. Susha and A. L. Rogach, *J. Phys. Chem. C*, 2007, **111**, 14889.
47 J. Cao, J. Z. Sun, J. Hong, H. Y. Li, H. Z. Chen and M. Wang, *Adv. Mater.*, 2004, **16**, 84.
48 L. Q. Jing, B. F. Xin, F. L. Yuan, L. P. Xue, B. Q. Wang and H. G. Fu, *J. Phys. Chem. B*, 2006, **110**, 17860.
49 X. H. Li, J. Niu, J. Zhang, H. L. Li and Z. F. Liu, *J. Phys. Chem. B*, 2003, **107**, 2453.
50 T. W. Ebbesen, H. Hiura, M. E. Bisher, M. M. J. Treacy, J. L. Shreeve-Keyer and R. C. Haushalter, *Adv. Mater.*, 1996, **8**, 155.
51 B. R. Azamian, K. S. Coleman, J. J. Davis, N. Hanson and M. L. H. Green, *Chem. Commun.*, 2002, 366.
52 S. Banerjee and S. S. Wong, *Nano Lett.*, 2002, **2**, 195.
53 N. Cho, K. R. Choudhury, R. B. Thapa, Y. Sahoo, T. Ohulchanskyy, A. N. Cartwright, K. S. Lee and P. N. Prasad, *Adv. Mater.*, 2007, **19**, 232.
54 M. J. Moghaddam, S. Taylor, M. Gao, S. M. Huang, L. M. Dai and M. J. McCall, *Nano Lett.*, 2004, **4**, 89.
55 M. Bottini, F. Cerignoli, M. I. Dawson, A. Magrini, N. Rosato and T. Mustelin, *Biomacromolecules*, 2006, **7**, 2259.
56 S. Ravindran, K. N. Bozhilov and C. S. Ozkan, *Carbon*, 2004, **42**, 1537.
57 K. S. Coleman, S. R. Bailey, S. Fogden and M. L. H. Green, *J. Am. Chem. Soc.*, 2003, **125**, 8722.
58 J. M. Haremza, M. A. Hahn and T. D. Krauss, *Nano Lett.*, 2002, **2**, 1253.
59 N. Chopra, M. Majumder and B. J. Hinds, *Adv. Funct. Mater.*, 2005, **15**, 858.
60 B. Pan, D. Cui, C. S. Ozkan, M. Ozkan, P. Xu, T. Huang, F. Liu, H. Chen, Q. Li, R. He and F. Gao, *J. Phys. Chem. C*, 2008, **112**, 939.
61 J. P. Zhang, Y. Liu, Y. G. Ke and H. Yan, *Nano Lett.*, 2006, **6**, 248.
62 X. G. Han, Y. L. Li and Z. X. Deng, *Adv. Mater.*, 2007, **19**, 1518.
63 T. Smorodin, U. Beierlein and J. P. Kotthaus, *Nanotechnology*, 2005, **16**, 1123.
64 K. Kurppa, H. Jiang, G. R. Szilvay, A. G. Nasibulin, E. L. Kauppinen and M. B. Linder, *Angew. Chem., Int. Ed.*, 2007, **46**, 6446.
65 M. Li, E. Dujardin and S. Mann, *Chem. Commun.*, 2005, 4952.
66 N. G. Portney, K. Singh, S. Chaudhary, G. Destito, A. Schneemann, M. Manchester and M. Ozkan, *Langmuir*, 2005, **21**, 2098.
67 M. E. Itkis, S. Niyogi, M. E. Meng, M. A. Hamon, H. Hu and R. C. Haddon, *Nano Lett.*, 2002, **2**, 155.
68 S. Chaudhary, J. H. Kim, K. V. Singh and M. Ozkan, *Nano Lett.*, 2004, **4**, 2415.
69 K. Y. Jiang, A. Eitan, L. S. Schadler, P. M. Ajayan, R. W. Siegel, N. Grobert, M. Mayne, M. Reyes-Reyes, H. Terrones and M. Terrones, *Nano Lett.*, 2003, **3**, 275.
70 L. Wang, S. J. Guo, L. J. Huang and S. J. Dong, *Electrochem. Commun.*, 2007, **9**, 827.
71 F. Stoffelbach, A. Aqil, C. Jerome, R. Jerome and C. Detrembleur, *Chem. Commun.*, 2005, 4532.
72 B. Kim and W. M. Sigmund, *Langmuir*, 2004, **20**, 8239.
73 A. Carrillo, J. A. Swartz, J. M. Gamba, R. S. Kane, N. Chakrapani, B. Q. Wei and P. M. Ajayan, *Nano Lett.*, 2003, **3**, 1437.
74 S. Hrapovic, Y. L. Liu, K. B. Male and J. H. T. Luong, *Anal. Chem.*, 2004, **76**, 1083.
75 Y. Liu, S. Wu, H. X. Ju and L. Xu, *Electroanalysis*, 2007, **19**, 986.
76 W. Li, C. Gao, H. Qian, J. Ren and D. Yan, *J. Mater. Chem.*, 2006, **16**, 1852.
77 M. Olek, M. Hilgendorff and M. Giersig, *Colloids Surf., A*, 2007, **292**, 83.
78 M. Olek, T. Biisgen, M. Hilgendorff and M. Giersig, *J. Phys. Chem. B*, 2006, **110**, 12901.
79 M. Grzelczak, M. A. Correa-Duarte, V. Salgueirino-Maceira, M. Giersig, R. Diaz and L. M. Liz-Marzan, *Adv. Mater.*, 2006, **18**, 415.
80 M. A. Correa-Duarte, N. Sobal, L. M. Liz-Marzan and M. Giersig, *Adv. Mater.*, 2004, **16**, 2179.
81 M. A. Correa-Duarte, J. Perez-Juste, A. Sanchez-Iglesias, M. Giersig and L. M. Liz-Marzan, *Angew. Chem., Int. Ed.*, 2005, **44**, 4375.
82 G. M. A. Rahman, D. M. Guldi, E. Zambon, L. Pasquato, N. Tagmatarchis and M. Prato, *Small*, 2005, **1**, 527.
83 J. B. Cui, C. P. Daghlian and U. J. Gibson, *J. Phys. Chem. B*, 2005, **109**, 11456.
84 L. Han, W. Wu, F. L. Kirk, J. Luo, M. M. Maye, N. N. Kariuki, Y. H. Lin, C. M. Wang and C. J. Zhong, *Langmuir*, 2004, **20**, 6019.
85 T. Sainsbury, J. Stolarczyk and D. Fitzmaurice, *J. Phys. Chem. B*, 2005, **109**, 16310.
86 A. V. Ellis, K. Vijayamohanan, R. Goswami, N. Chakrapani, L. S. Ramanathan, P. M. Ajayan and G. Ramanath, *Nano Lett.*, 2003, **3**, 279.
87 X. L. Li, Y. Q. Liu, L. Fu, L. C. Cao, D. C. Wei, G. Yu and D. B. Zhu, *Carbon*, 2006, **44**, 3139.
88 S. Fullam, D. Cottell, H. Rensmo and D. Fitzmaurice, *Adv. Mater.*, 2000, **12**, 1430.
89 T. Sainsbury and D. Fitzmaurice, *Chem. Mater.*, 2004, **16**, 3780.
90 T. Sainsbury and D. Fitzmaurice, *Chem. Mater.*, 2004, **16**, 2174.
91 D. Q. Yang, B. Hennequin and E. Sacher, *Chem. Mater.*, 2006, **18**, 5033.
92 Z. Wang, M. Li, Y. Zhang, J. Yuan, Y. Shen, L. Niu and A. Ivaska, *Carbon*, 2007, **45**, 2111.
93 X. Li, Y. Liu, L. Fu, L. Cao, D. Wei and Y. Wang, *Adv. Funct. Mater.*, 2006, **16**, 2431.
94 L. Liu, J. X. Li, Z. X. Guo, L. M. Dai, D. Q. Zhang and D. B. Zhu, *Chem. Phys. Lett.*, 2003, **367**, 747.
95 Y. Y. Ou and M. H. Huang, *J. Phys. Chem. B*, 2006, **110**, 2031.
96 V. Georgakilas, V. Tzitzios, D. Gournis and D. Petridis, *Chem. Mater.*, 2005, **17**, 1613.
97 D. M. Guldi, G. M. A. Rahman, V. Sgobba, N. A. Kotov, D. Bonifazi and M. Prato, *J. Am. Chem. Soc.*, 2006, **128**, 2315.
98 Y. Y. Mu, H. P. Liang, J. S. Hu, L. Jiang and L. J. Wan, *J. Phys. Chem. B*, 2005, **109**, 22212.
99 H. C. Choi, M. Shim, S. Bangsaruntip and H. J. Dai, *J. Am. Chem. Soc.*, 2002, **124**, 9058.
100 B. S. Kong, D. H. Jung, S. K. Oh, C. S. Han and H. T. Jung, *J. Phys. Chem. C*, 2007, **111**, 8377.
101 L. T. Qu and L. M. Dai, *J. Am. Chem. Soc.*, 2005, **127**, 10806.
102 L. T. Qu, L. M. Dai and E. Osawa, *J. Am. Chem. Soc.*, 2006, **128**, 5523.
103 Y. Lee, H. J. Song, H. S. Shin, H. J. Shin and H. C. Choi, *Small*, 2005, **1**, 975.
104 C. Gao, W. W. Li, Y. Z. Jin and H. Kong, *Nanotechnology*, 2006, **17**, 2882.
105 J. Y. Cao, C. Du, S. C. C. Wang, P. Mercier, X. G. Zhang, H. Yang and D. L. Akins, *Electrochem. Commun.*, 2007, **9**, 735.
106 X. Lu and T. Imae, *J. Phys. Chem. C*, 2007, **111**, 2416.
107 S. Banerjee and S. S. Wong, *Chem. Commun.*, 2004, 1866.
108 S. Banerjee and S. S. Wong, *J. Am. Chem. Soc.*, 2003, **125**, 10342.
109 I. Robel, B. A. Bunker and P. V. Kamat, *Adv. Mater.*, 2005, **17**, 2458.
110 L. Zhao and L. Gao, *J. Mater. Chem.*, 2004, **14**, 1001.
111 D. S. Yu, Y. J. Chen, B. J. Li, X. D. Chen and M. Q. Zhang, *Appl. Phys. Lett.*, 2007, **90**, 161103.
112 S. Banerjee and S. S. Wong, *Nano Lett.*, 2004, **4**, 1445.
113 S. Banerjee, T. Hemraj-Benny, M. Balasubramanian, D. Fischer, J. A. Misewich and S. S. Wong, *Chem. Commun.*, 2004, 772.
114 B. H. Juarez, C. Klinke, A. Kornowski and H. Weller, *Nano Lett.*, 2007, **7**, 3564.
115 F. Gu, C. Z. Li and S. F. Wang, *Inorg. Chem.*, 2007, **46**, 5343.
116 S. W. Lee and W. M. Sigmund, *Chem. Commun.*, 2003, 780.
117 G. Guo, J. Guo, D. Tao, W. C. H. Choy, L. Zhao, W. Qian and Z. Wang, *Appl. Phys. A*, 2007, **89**, 525.
118 C. H. Tseng and C. Y. Chen, *Nanotechnology*, 2008, **19**, 035606.
119 W. Q. Han and A. Zettl, *Nano Lett.*, 2003, **3**, 681.
120 X. H. Xia, Z. H. Jia, Y. Yu, Y. Liang, Z. Wang and L. L. Ma, *Carbon*, 2007, **45**, 717.
121 B. Xue, P. Chen, Q. Hong, J. Y. Lin and K. L. Tan, *J. Mater. Chem.*, 2001, **11**, 2378.
122 R. Q. Yu, L. W. Chen, Q. P. Liu, J. Y. Lin, K. L. Tan, S. C. Ng, H. S. O. Chan, G. Q. Xu and T. S. A. Hor, *Chem. Mater.*, 1998, **10**, 718.

 This journal is © The Royal Society of Chemistry 2009

Published on 13 February 2009. Downloaded by Pennsylvania State University on 12/09/2016 18:00:11.

123 Y. H. Lin, X. L. Cui, C. Yen and C. M. Wai, *J. Phys. Chem. B*, 2005, **109**, 14410.
124 X. R. Ye, Y. H. Lin, C. M. Wang, M. H. Engelhard, Y. Wang and C. M. Wai, *J. Mater. Chem.*, 2004, **14**, 908.
125 J. P. Hu, J. H. Shi, S. P. Li, Y. J. Qin, Z. X. Guo, Y. L. Song and D. B. Zhu, *Chem. Phys. Lett.*, 2005, **401**, 352.
126 M. N. Zhang, L. Su and L. Q. Mao, *Carbon*, 2006, **44**, 276.
127 D. Wang, Z. C. Li and L. W. Chen, *J. Am. Chem. Soc.*, 2006, **128**, 15078.
128 R. Zanella, E. V. Basiuk, P. Santiago, V. A. Basiuk, E. Mireles, I. Puente-Lee and J. M. Saniger, *J. Phys. Chem. B*, 2005, **109**, 16290.
129 P. Chen, X. Wu, J. Lin and K. L. Tan, *J. Phys. Chem. B*, 1999, **103**, 4559.
130 Z. Y. Sun, Z. M. Liu, B. X. Han, S. D. Miao, Z. J. Miao and G. M. An, *J. Colloid Interface Sci.*, 2006, **304**, 323.
131 Z. Y. Sun, Z. M. Liu, B. X. Han, Y. Wang, J. Du, Z. Xie and G. Han, *Adv. Mater.*, 2005, **17**, 928.
132 R. Giordano, P. Serp, P. Kalck, Y. Kihn, J. Schreiber, C. Marhic and J. L. Duvail, *Eur. J. Inorg. Chem.*, 2003, 610.
133 Y.-T. Kim, K. Ohshima, K. Higashimine, T. Uruga, M. Takata, H. Suematsu and T. Mitani, *Angew. Chem., Int. Ed.*, 2006, **45**, 407.
134 R. Y. Zhang and X. M. Wang, *Chem. Mater.*, 2007, **19**, 976.
135 W. X. Chen, J. Y. Lee and Z. Liu, *Mater. Lett.*, 2004, **58**, 3166.
136 W. Z. Li, C.H. Liang, W. J. Zhou, J. S. Qiu, Z. H. Zhou, G. Q. Sun and Q. Xin, *J. Phys. Chem. B*, 2003, **107**, 6292.
137 C. C. Chien and K. T. Jeng, *Mater. Chem. Phys.*, 2006, **99**, 80.
138 B. P. Jia and L. Gao, *J. Phys. Chem. B*, 2007, **111**, 5337.
139 Y. Shan and L. Gao, *J. Am. Ceram. Soc.*, 2006, **89**, 759.
140 V. Tzitzios, V. Georgakilas, E. Oikonomou, M. Karakassides and D. Petridis, *Carbon*, 2006, **44**, 848.
141 A. Kongkanand, K. Vinodgopal, S. Kuwabata and P. V. Kamat, *J. Phys. Chem. B*, 2006, **110**, 16185.
142 X. G. Hu, T. Wang, X. H. Qu and S. J. Dong, *J. Phys. Chem. B*, 2006, **110**, 853.
143 D. J. Guo and H. L. Li, *J. Electroanal. Chem.*, 2004, **573**, 197.
144 G. G. Wildgoose, C. E. Banks and R. G. Compton, *Small*, 2006, **2**, 182.
145 D. J. Guo and H. L. Li, *Electrochem. Commun.*, 2004, **6**, 999.
146 D. J. Guo and H. L. Li, *J. Colloid Interface Sci.*, 2005, **286**, 274.
147 B. M. Quinn, C. Dekker and S. G. Lemay, *J. Am. Chem. Soc.*, 2005, **127**, 6146.
148 H. F. Cui, J. S. Ye, W. D. Zhang, J. Wang and F. S. Sheu, *J. Electroanal. Chem.*, 2005, **577**, 295.
149 T. M. Day, P. R. Unwin, N. R. Wilson and J. V. Macpherson, *J. Am. Chem. Soc.*, 2005, **127**, 10639.
150 M. Kalbac, O. Frank, L. Kavan, M. Zukalova, J. Prochazka, M. Klementova and L. Dunsch, *J. Electrochem. Soc.*, 2007, **154**, K19.
151 S. V. Mahajan, S. A. Hasan, J. Cho, M. S. P. Shaffer, A. R. Boccaccini and J. H. Dickerson, *Nanotechnology*, 2008, **19**, 195301.
152 Y. Liu, J. Chen, W. M. Zhang, Z. F. Ma, G. F. Swiegers, C. O. Too and G. G. Wallace, *Chem. Mater.*, 2008, **20**, 2603.
153 Y. C. Xing, *J. Phys. Chem. B*, 2004, **108**, 19255.
154 B. C. Satishkumar, E. M. Vogl, A. Govindaraj and C. N. R. Rao, *J. Phys. D: Appl. Phys.*, 1996, **29**, 3173.
155 A. Fasi, I. Palinko, J. W. Seo, Z. Konya, K. Hernadi and I. Kiricsi, *Chem. Phys. Lett.*, 2003, **372**, 848.
156 L. Qiu, V. G. Pol, Y. Wei and A. Gedanken, *New J. Chem.*, 2004, **28**, 1056.
157 M. S. Raghuveer, S. Agrawal, N. Bishop and G. Ramanath, *Chem. Mater.*, 2006, **18**, 1390.
158 Y. Wang, X. Xu, Z. Q. Tian, Y. Zong, H. M. Cheng and C. J. Lin, *Chem.–Eur. J.*, 2006, **12**, 2542.
159 H. Yu, X. Quan, S. Chen and H. Zhao, *J. Phys. Chem. C*, 2007, **111**, 12987.
160 D. Mattia, G. Korneva, A. Sabur, G. Friedman and Y. Gogotsi, *Nanotechnology*, 2007, **18**, 155305/1.
161 W. K. Wong, S. H. Lim and J. T. L. Thong, *Nanotechnology*, 2006, **17**, 2373.
162 G. H. Lu, L. Y. Zhu, P. X. Wang, J. H. Chen, D. A. Dikin, R. S. Ruoff, Y. Yu and Z. F. Ren, *J. Phys. Chem. C*, 2007, **111**, 17919.
163 J. Chen and G. Lu, *Nanotechnology*, 2006, **17**, 2891.
164 M. S. Raghuveer, A. Kumar, M. J. Frederick, G. P. Louie, P. G. Ganesan and G. Ramanath, *Adv. Mater.*, 2006, **18**, 547.
165 L. Q. Jiang and L. Gao, *Mater. Chem. Phys.*, 2005, **91**, 313.
166 J. M. Planeix, N. Coustel, B. Coq, V. Brotons, P. S. Kumbhar, R. Dutartre, P. Geneste, P. Bernier and P. M. Ajayan, *J. Am. Chem. Soc.*, 1994, **116**, 7935.
167 G. Girishkumar, M. Rettker, R. Underhile, D. Binz, K. Vinogopal, P. McGinn and P. Kamat, *Langmuir*, 2005, **21**, 8487.
168 A. Kongkanand, S. Kuwabata, G. Girishkumar and P. Kamat, *Langmuir*, 2006, **22**, 2392.
169 J. Li, Y. J. Lu, Q. Ye, M. Cinke, J. Han and M. Meyyappan, *Nano Lett.*, 2003, **3**, 929.
170 Q. Zhao, M. B. Nardelli, W. Lu and J. Bernholc, *Nano Lett.*, 2005, **5**, 847.
171 R. Wang, D. Zhang, W. Sun, Z. Han and C. Liu, *J. Mol. Struct.*, 2007, **806**, 93.
172 J. X. Zhao and Y. H. Ding, *Mater. Chem. Phys.*, 2008, **110**, 411.
173 J. Kong, M. G. Chapline and H. Dai, *Adv. Mater.*, 2001, **13**, 1384.
174 S. Mubeen, T. Zhang, B. Yoo, M. A. Deshusses and N. V. Myung, *J. Phys. Chem. C*, 2007, **111**, 6321.
175 Y. Sun and H. H. Wang, *Appl. Phys. Lett.*, 2007, **90**, 213107.
176 Y. J. Lu, J. Li, J. Han, H. T. Ng, C. Binder, C. Partridge and M. Meyyappan, *Chem. Phys. Lett.*, 2004, **391**, 344.
177 Y. Li, H. C. Wang, Y. S. Chen and M. J. Yang, *Sens. Actuators, B*, 2008, **132**, 155.
178 X. Ji, C. E. Banks, A. F. Holloway, K. Jurkschat, C. A. Thorogood, G. G. Wildgoose and R. G. Compton, *Electroanalysis*, 2006, **18**, 2481.
179 A. Star, V. Joshi, S. Skarupo, D. Thomas and J. P. Gabriel, *J. Phys. Chem. B*, 2006, **110**, 21014.
180 P. Young, Y. Lu, R. Terrill and J. Li, *J. Nanosci. Nanotechnol.*, 2005, **5**, 1509.
181 Z. M. Qi, M. Wei, I. Honma and H. Zhou, *ChemPhysChem*, 2007, **8**, 264.
182 S. Chen, R. Yuan, Y. Chai, L. Zhang, N. Wang and X. Li, *Biosens. Bioelectron.*, 2007, **22**, 1268.
183 G. Nair and M. G. Bawendi, *Phys. Rev. B*, 2007, **76**, 081304.
184 R. D. Schaller, V. M. Agranovich and V. I. Klimov, *Nat. Phys.*, 2005, **1**, 189.
185 R. D. Schaller and V. I. Klimov, *Phys. Rev. Lett.*, 2004, **92**, 186601/1.
186 R. D. Schaller and V. I. Klimov, *Phys. Rev. Lett.*, 2006, **96**, 097402/1.
187 C. Berger, Y. Yi, Z. L. Wang and W. A. de Heer, *Appl. Phys. A*, 2002, **74**, 363.
188 S. J. Wind, J. Appenzeller and P. Avouris, *Phys. Rev. Lett.*, 2003, **91**, 058301/1.
189 A. Javey, J. Guo, Q. Wang, M. Lundstrom and H. J. Dai, *Nature*, 2003, **424**, 654.
190 S. Ravindran, S. Chaudhary, B. Colburn, M. Ozkan and C. S. Ozkan, *Nano Lett.*, 2003, **3**, 447.
191 D. Noy, C. C. Moser and P. L. Dutton, *Biochim. Biophys. Acta*, 2006, **1757**, 90.
192 F. Vietmeyer, B. Seger and P. V. Kamat, *Adv. Mater.*, 2007, **19**, 2935.
193 L. Sheeney-Haj-Khia, B. Basnar and I. Willner, *Angew. Chem., Int. Ed.*, 2005, **44**, 78.
194 A. Kongkanand, R. M. Dominguez and P. V. Kamat, *Nano Lett.*, 2007, **7**, 676.
195 A. Kongkanand and P. V. Kamat, *ACS Nano*, 2007, **1**, 13.
196 P. Brown, K. Takechi and P. V. Kamat, *J. Phys. Chem. C*, 2008, **112**, 4776.
197 L. Hu, Y. L. Zhao, K. Ryu, C. Zhou, J. F. Stoddart and G. Gruner, *Adv. Mater.*, 2008, **20**, 939.
198 B. J. Landi, S. L. Castro, H. J. Ruf, C. M. Evans, S. G. Bailey and R. P. Raffaelle, *Sol. Energy Mater. Sol. Cells*, 2005, **87**, 733.
199 N. W. S. Kam and H. Dai, *J. Am. Chem. Soc.*, 2005, **127**, 6021.
200 N. W. S. Kam and H. Dai, *Phys. Status Solidi B*, 2006, **243**, 3561.
201 N. W. S. Kam, T. C. Jessop, P. A. Wender and H. Dai, *J. Am. Chem. Soc.*, 2004, **126**, 6850.
202 N. W. S. Kam, Z. Liu and H. Dai, *J. Am. Chem. Soc.*, 2005, **127**, 12492.
203 N. W. S. Kam, Z. Liu and H. Dai, *Angew. Chem., Int. Ed.*, 2006, **45**, 577.

Published on 13 February 2009. Downloaded by Pennsylvania State University on 12/09/2016 18:00:11.

204 N. W. S. Kam, M. O'Connell, J. A. Wisdom and H. Dai, *Proc. Natl. Acad. Sci. U. S. A.*, 2005, **102**, 11600.
205 G. Pastorin, K. Kostarelos, M. Prato and A. Bianco, *J. Biomed. Nanotechnol.*, 2005, **1**, 133.
206 V. Georgakilas, N. Tagmatarchis, D. Pantarotto, A. Bianco, J.-P. Briand and M. Prato, *Chem. Commun.*, 2002, 3050.
207 D. Pantarotto, J.-P. Briand, M. Prato and A. Bianco, *Chem. Commun.*, 2004, 16.
208 D. Pantarotto, C. D. Partidos, R. Graff, J. Hoebeke, J.-P. Briand, M. Prato and A. Bianco, *J. Am. Chem. Soc.*, 2003, **125**, 6160.
209 D. Pantarotto, C. D. Partidos, J. Hoebeke, F. Brown, E. Kramer, J.-P. Briand, S. Muller, M. Prato and A. Bianco, *Chem. Biol.*, 2003, **10**, 961.
210 D. Pantarotto, R. Singh, D. McCarthy, M. Erhardt, J.-P. Briand, M. Prato, K. Kostarelos and A. Bianco, *Angew. Chem., Int. Ed.*, 2004, **43**, 5242.
211 L. Lacerda, A. Bianco, M. Prato and K. Kostarelos, *J. Mater. Chem.*, 2008, **18**, 17.
212 R. Singh, D. Pantarotto, D. McCarthy, O. Chaloin, J. Hoebeke, C. D. Partidos, J.-P. Briand, M. Prato, A. Bianco and K. Kostarelos, *J. Am. Chem. Soc.*, 2005, **127**, 4388.
213 A. Bianco, J. Hoebeke, S. Godefroy, O. Chaloin, D. Pantarotto, J.-P. Briand, S. Muller, M. Prato and C. D. Partidos, *J. Am. Chem. Soc.*, 2005, **127**, 58.
214 W. Wu, S. Wieckowski, G. Pastorin, M. Benincasa, C. Klumpp, J.-P. Briand, R. Gennaro, M. Prato and A. Bianco, *Angew. Chem., Int. Ed.*, 2005, **44**, 6358.
215 K. Kostarelos, L. Lacerda, G. Pastorin, W. Wu, S. Wieckowski, J. Luangsivilay, S. Godefroy, D. Pantarotto, J.-P. Briand, S. Muller, M. Prato and A. Bianco, *Nat. Nanotechnol.*, 2007, **2**, 108.
216 W. C. W. Chan, D. J. Maxwell, X. Gao, R. E. Bailey, M. Han and S. Nie, *Curr. Opin. Chem. Biol.*, 2002, **13**, 40.
217 M. Bruchez Jr, M. Moronne, P. Gin, S. Weiss and A. P. Alivisatos, *Science*, 1998, **281**, 2013.
218 J. H. Choi, F. T. Nguyen, P. W. Barone, D. A. Heller, A. E. Moll, D. Patel, S. A. Boppart and M. S. Strano, *Nano Lett.*, 2007, **7**, 861.
219 N. Q. Jia, Q. Lian, H. B. Shen, C. Wang, X. Y. Li and Z. N. Yang, *Nano Lett.*, 2007, **7**, 2976.
220 A. L. M. Reddy and S. Ramaprabhu, *J. Phys. Chem. C*, 2007, **111**, 7727.
221 J. Li, S. Tang, L. Lu and H. C. Zeng, *J. Am. Chem. Soc.*, 2007, **129**, 9401.

 This journal is © The Royal Society of Chemistry 2009